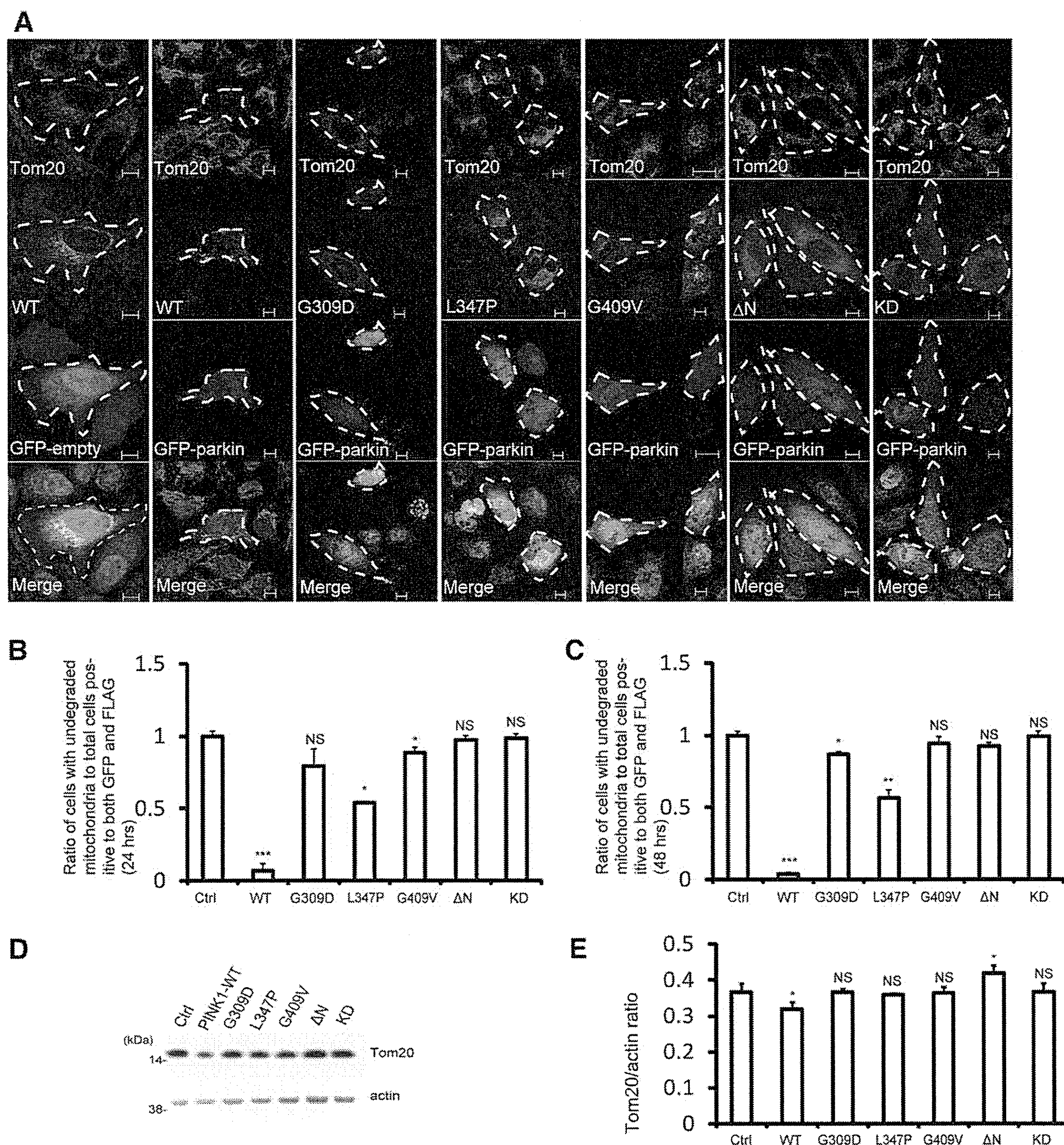

Fig. 4. PINK1 mutants remain diffusely distributed and are not recruited to mitochondria, resulting in reduced mitochondrial elimination. (A) Immunocytochemistry of HeLa cells transiently overexpressing GFP-empty vector and PINK1-3xFLAG (WT) as control, and GFP-parkin and PINK1-3xFLAG (WT or various mutants), 48 h after transfection. Tom20, WT and PINK1 mutants, or GFP are in red, white, or green, respectively. Bars, 10 μm. (B and C) Ratio of cells with undegraded mitochondria to total cells positive for both GFP and FLAG, 24 h (B) and 48 h (C) after transfection are shown in the graph. (D) Levels of Tom20 in HeLa cells transiently overexpressing GFP-empty vector and PINK1-3xFLAG (WT), and GFP-parkin and PINK1-3xFLAG (WT or various mutants) were analyzed with immunoblotting. (E) Quantification of (D); error bars indicate standard deviation of at least three experiments. $^{*}P < 0.05$, $^{**}P < 0.01$, $^{***}P < 0.001$. NS, non-significant.

kinase activity and mitochondrial localization of PINK1 are indispensable for mitochondrial elimination.

3.5. Overexpression of wild-type PINK1 in combination with parkin induces mitophagy

Very recently, it has been reported aggregated mitochondria in cells overexpressing both PINK1 and parkin colocalize with lysosomes as well as autophagosomes [9]. However, the fate of perinuclear aggregated mitochondria has not been examined. Therefore, we checked whether PINK1–parkin dependent mitochondrial elimination was dependent on mitophagy. Mitochondrial elimination was enhanced by overexpression of PINK1 with parkin in wild-type MEFs. On the other hand, $Atg7^{-/-}$ MEFs, which lack a key component of the autophagy system, retain expression of Tom20 (Fig. 5A and B). To further analyze this hypothesis, we examined the change of endogenous LC3 distribution following both PINK1 and parkin overexpression. We confirmed accumulation of parkin, which overlaps with aggregated mitochondria (refer to Fig. 3), in cells expressing both wild-type proteins. Likewise, endogenous LC3 mainly colocalized with wild-type PINK1, adjoined to the outer mitochondrial membrane, but did not colocalize with G409V or ΔN

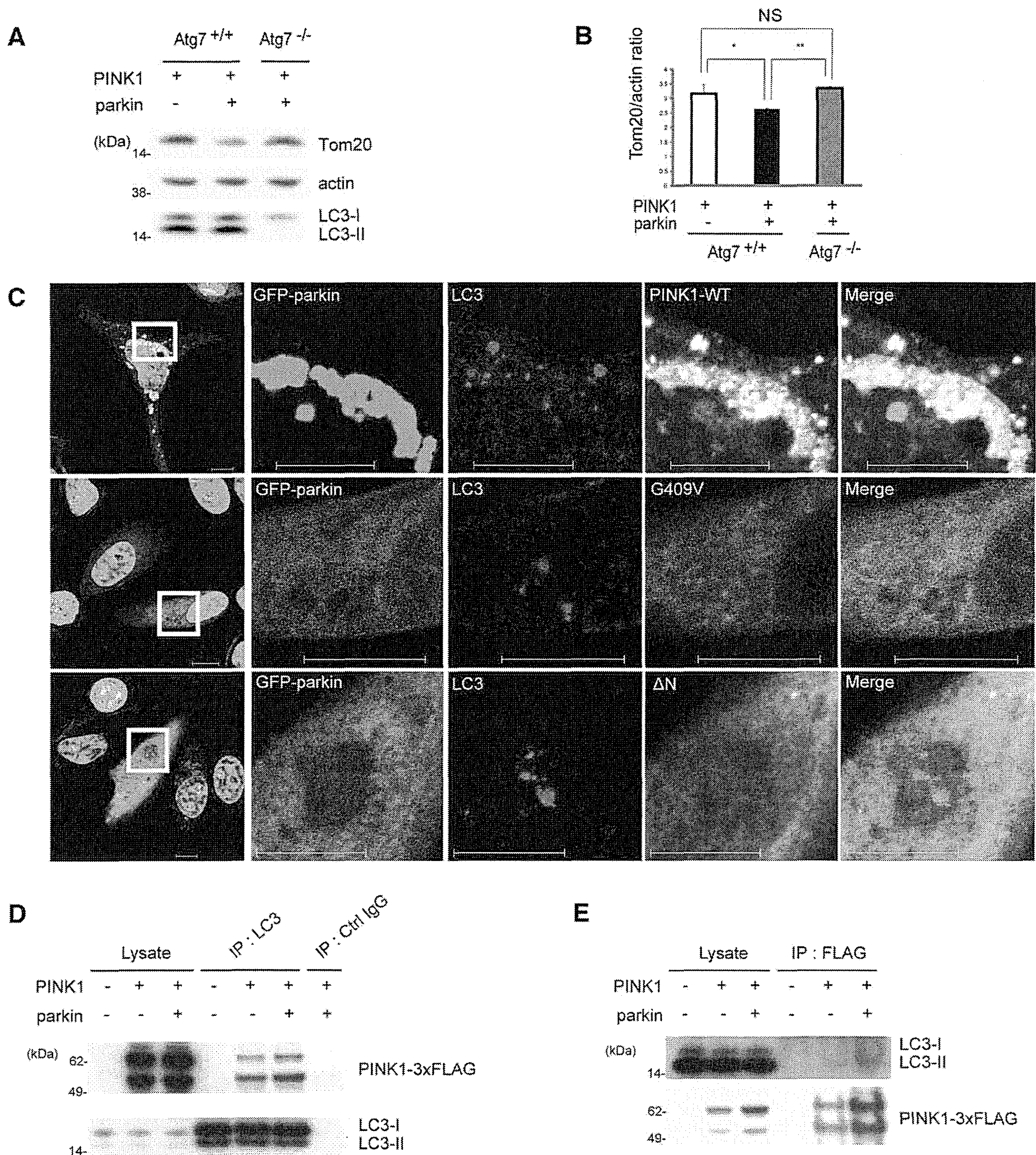

Fig. 5. Overexpression of wild-type PINK1 in combination with parkin induces mitophagy. (A) Levels of Tom20 in Atg7$^{+/+}$ MEFs overexpressing GFP-empty vector and PINK1-3xFLAG and those in Atg7$^{+/+}$ and Atg7$^{-/-}$ MEFs overexpressing GFP-parkin and PINK1-3xFLAG, 48 h after transfection were analyzed by immunoblotting. (B) Quantification of (A); error bars indicate standard deviation of at least three experiments. $^{*}P < 0.05$, $^{**}P < 0.01$, NS, non-significant. (C) Immunocytochemistry of HeLa cells transiently overexpressing GFP-parkin and PINK1-3xFLAG (wild-type, G409V, and ΔN), 24 h after transfection. PINK1 (WT and mutants), LC3, or GFP-parkin are in white, red, or green, respectively. The boxed areas are shown in the three right-hand images at a higher magnification. Bars, 10 μm. (D and E) HeLa cells overexpressing 3xFLAG-empty vector and GFP-empty vector, PINK1-3xFLAG and GFP-empty vector, or PINK1-3xFLAG and GFP-parkin, 24 h after transfection were immunoprecipitated with anti-LC3 antibodies (D) or anti-FLAG antibodies (E) and immunoblotted for FLAG or LC3. Immunoblotting of total lysates was performed to test the expression levels. IP, immunoprecipitation.

(Fig. 5C), nor with G309D, L347P and KD (data not shown). LC3 also partially colocalized with parkin. Compared with Fig. 1D, the colocalization of endogenous LC3 with PINK1 was markedly enhanced. Next, to investigate direct interaction, cell lysates were immunoprecipitated using anti-LC3 antibodies and immunoblotted with anti-FLAG antibodies (Fig. 5D). The reverse immunoprecipitation was also performed (Fig. 5E). These results allowed us to conclude that PINK1 binds with LC3-II. Taken together, we concluded that mitochondrial elimination by the PINK1–parkin pathway is dependent on mitochondrial autophagic activity.

In this study, we have found that overexpression of both proteins enhances mitochondrial elimination via autophagy. In

contrast to the results of a *Drosophila* study, a PINK1–parkin pathway promotes mitochondrial enlargement or aggregation in mammalian cellular models [8,18]. However, only PINK1 overexpressing cells exhibit longer mitochondria with increased interconnectivity, but the abnormal mitochondria do not elicit an autophagic response [12]. Consistent with this, wild-type PINK1 overexpression did not change the level of endogenous LC3-II (data not shown). Therefore, coordinating activation of parkin and PINK1 contributes to mitophagy.

PINK1 localization in mitochondria is dependent on its MTS region and it exhibits autophosphorylation activity in vitro [2,13,14]. Parkin is recognized as an in vivo substrate of PINK1 and parkin site-direct phosphorylation by wild-type PINK1 is critical for the translocation of parkin into the mitochondria in cellular and *Drosophila* models [8]. In agreement with this report, our study showed that parkin recruitment to the mitochondria by PINK1 was dependent on PINK1 kinase activity.

Silencing of PINK1 with shRNA increased mitochondrial fission and induced mitophagy [12]. Although PINK1 overexpression is protective against oxidative stress-induced apoptotic cell death [2,19,20], excess wild-type PINK1 without parkin overexpression does not elicit mitochondrial autophagy [12]. Our immunocytochemical experiments revealed that PINK1 co-overexpressed with parkin colocalized mainly with LC3-positive vesicles and partially with perinuclear aggregated mitochondria, which were expected to colocalize with aggregated parkin. In addition, molecular binding between PINK1 and LC3-II was confirmed by immunoprecipitation, which suggests that association between PINK1 and LC3 contribute to mitophagy. Combined with the observation by Vives-Bausa et al., although it is not clear whether an excess of mitophagy would be harmful to cells, a PINK1–parkin pathway, which is regulated by kinase activity and/or the mitochondrial localization of PINK1, would control mitochondrial maintenance via the autophagic machinery.

Acknowledgments

We thank Drs. Masaaki Komatsu and Yu-shin Sou (Laboratory of Frontier Science, Tokyo Metropolitan Institute of Medical Science) for providing $Atg7^{-/-}$ MEFs and Hattori's laboratory members for helpful discussions. We are grateful to Drs. Junichi Nakamoto, Yoko Imamichi, and Akiko Egashira for technical assistance. This study was supported by a Young Scientist Grant (F.S. and S. Saiki), an All Japan Coffee Association Grant (S. Saiki), a Takeda Scientific Association Grant (S. Saiki) and a Grant from Nagao Memorial Fund (S. Saiki).

References

[1] Abou-Sleiman, P.M., Muqit, M.M. and Wood, N.W. (2006) Expanding insights of mitochondrial dysfunction in Parkinson's disease. Nat. Rev. Neurosci. 7, 207–219.

[2] Valente, E.M. et al. (2004) Hereditary early-onset Parkinson's disease caused by mutations in PINK1. Science 304, 1158–1160.

[3] Clark, I.E. et al. (2006) Drosophila pink1 is required for mitochondrial function and interacts genetically with parkin. Nature 441, 1162–1166.

[4] Park, J. et al. (2006) Mitochondrial dysfunction in Drosophila PINK1 mutants is complemented by parkin. Nature 441, 1157–1161.

[5] Yang, Y., Ouyang, Y., Yang, L., Beal, M.F., McQuibban, A., Vogel, H. and Lu, B. (2008) Pink1 regulates mitochondrial dynamics through interaction with the fission/fusion machinery. Proc. Natl. Acad. Sci. USA 105, 7070–7075.

[6] Twig, G. et al. (2008) Fission and selective fusion govern mitochondrial segregation and elimination by autophagy. EMBO J. 27, 433–446.

[7] Narendra, D., Tanaka, A., Suen, D.F. and Youle, R.J. (2008) Parkin is recruited selectively to impaired mitochondria and promotes their autophagy. J. Cell Biol. 183, 795–803.

[8] Kim, Y. et al. (2008) PINK1 controls mitochondrial localization of Parkin through direct phosphorylation. Biochem. Biophys. Res. Commun. 377, 975–980.

[9] Vives-Bauza, C. et al. (2010) PINK1-dependent recruitment of Parkin to mitochondria in mitophagy. Proc. Natl. Acad. Sci. USA 107, 378–383.

[10] Kabeya, Y. et al. (2000) LC3, a mammalian homologue of yeast Apg8p, is localized in autophagosome membranes after processing. EMBO J. 19, 5720–5728.

[11] Hatano, T., Kubo, S., Imai, S., Maeda, M., Ishikawa, K., Mizuno, Y. and Hattori, N. (2007) Leucine-rich repeat kinase 2 associates with lipid rafts. Hum. Mol. Genet. 16, 678–690.

[12] Dagda, R.K., Cherra 3rd, S.J., Kulich, S.M., Tandon, A., Park, D. and Chu, C.T. (2009) Loss of PINK1 function promotes mitophagy through effects on oxidative stress and mitochondrial fission. J. Biol. Chem. 284, 13843–13855.

[13] Silvestri, L., Caputo, V., Bellacchio, E., Atorino, L., Dallapiccola, B., Valente, E.M. and Casari, G. (2005) Mitochondrial import and enzymatic activity of PINK1 mutants associated to recessive parkinsonism. Hum. Mol. Genet. 14, 3477–3492.

[14] Beilina, A., Van Der Brug, M., Ahmad, R., Kesavapany, S., Miller, D.W., Petsko, G.A. and Cookson, M.R. (2005) Mutations in PTEN-induced putative kinase 1 associated with recessive parkinsonism have differential effects on protein stability. Proc. Natl. Acad. Sci. USA 102, 5703–5708.

[15] Um, J.W., Stichel-Gunkel, C., Lubbert, H., Lee, G. and Chung, K.C. (2009) Molecular interaction between parkin and PINK1 in mammalian neuronal cells. Mol. Cell Neurosci. 40, 421–432.

[16] Hatano, Y. et al. (2004) Novel PINK1 mutations in early-onset parkinsonism. Ann. Neurol. 56, 424–427.

[17] Sim, C.H., Lio, D.S., Mok, S.S., Masters, C.L., Hill, A.F., Culvenor, J.G. and Cheng, H.C. (2006) C-terminal truncation and Parkinson's disease-associated mutations down-regulate the protein serine/threonine kinase activity of PTEN-induced kinase-1. Hum. Mol. Genet. 15, 3251–3262.

[18] Exner, N. et al. (2007) Loss-of-function of human PINK1 results in mitochondrial pathology and can be rescued by parkin. J. Neurosci. 27, 12413–12418.

[19] Petit, A. et al. (2005) Wild-type PINK1 prevents basal and induced neuronal apoptosis, a protective effect abrogated by Parkinson disease-related mutations. J. Biol. Chem. 280, 34025–34032.

[20] Pridgeon, J.W., Olzmann, J.A., Chin, L.S. and Li, L. (2007) PINK1 protects against oxidative stress by phosphorylating mitochondrial chaperone TRAP1. PLoS Biol. 5, e172.

BASIC RESEARCH PAPER

Autophagy 7:2, 1-12; February 2011; © 2011 Landes Bioscience

Caffeine induces apoptosis by enhancement of autophagy via PI3K/Akt/mTOR/p70S6K inhibition

Shinji Saiki,[1] Yukiko Sasazawa,[2] Yoko Imamichi,[1] Sumihiro Kawajiri,[1] Takahiro Fujimaki,[2] Isei Tanida,[3] Hiroki Kobayashi,[2] Fumiaki Sato,[4] Shigeto Sato,[1] Kei-Ichi Ishikawa,[1] Masaya Imoto[2] and Nobutaka Hattori[1,*]

[1]Department of Neurology; Juntendo University School of Medicine; Bunkyo, Tokyo; [2]Department of Biosciences and Informatics; Faculty of Science and Technology; Keio University; Kohoku, Yokohama; [3]Department of Biochemistry and Cell Biology; National Institute of Infectious Diseases; Shinjyuku, Tokyo; [4]Research Institute for Disease of Old Age; Juntendo University School of Medicine; Tokyo, Japan

Key words: apoptosis, autophagy, PI3K/Akt/mTOR/p70S6K, ERK1/2, caffeine

Abbreviations: PI3K, phosphoinositide-3 kinase; 4E-BP1, eukaryotic initiation factor 4-binding protein 1; ERK, extracellular signal-regulated kinase; mTOR, mammalian target of rapamycin; 3-MA, 3-methyladenine; MEFs, mouse embryonic fibroblasts; p70S6K, 70-kDa ribosomal protein S6 kinase; PI, propidium iodide; MPP+, 1-methyl-4-phenylpyridinium

Caffeine is one of the most frequently ingested neuroactive compounds. All known mechanisms of apoptosis induced by caffeine act through cell cycle modulation or p53 induction. It is currently unknown whether caffeine-induced apoptosis is associated with other cell death mechanisms, such as autophagy. Herein we show that caffeine increases both the levels of microtubule-associated protein 1 light chain 3-II and the number of autophagosomes, through the use of western blotting, electron microscopy and immunocytochemistry techniques. Phosphorylated p70 ribosomal protein S6 kinase (Thr389), S6 ribosomal protein (Ser235/236), 4E-BP1 (Thr37/46) and Akt (Ser473) were significantly decreased by caffeine. In contrast, ERK1/2 (Thr202/204) was increased by caffeine, suggesting an inhibition of the Akt/mTOR/p70S6K pathway and activation of the ERK1/2 pathway. Although insulin treatment phosphorylated Akt (Ser473) and led to autophagy suppression, the effect of insulin treatment was completely abolished by caffeine addition. Caffeine-induced autophagy was not completely blocked by inhibition of ERK1/2 by U0126. Caffeine induced reduction of mitochondrial membrane potentials and apoptosis in a dose-dependent manner, which was further attenuated by the inhibition of autophagy with 3-methyladenine or Atg7 siRNA knockdown. Furthermore, there was a reduced number of early apoptotic cells (annexin V positive, propidium iodide negative) among autophagy-deficient mouse embryonic fibroblasts treated with caffeine than in their wild-type counterparts. These results support previous studies on the use of caffeine in the treatment of human tumors and indicate a potential new target in the regulation of apoptosis.

Introduction

Caffeine has a diverse range of pharmacological effects.[1] In addition to its various effects on the cell cycle and growth arrest, higher (4–10 mM) concentrations of caffeine can induce apoptosis in several cell lines, such as 10 mM caffeine in human neuroblastoma cells,[2] 4 mM caffeine in human pancreatic adenocarcinoma cells[3] and 5 mM caffeine in human A549 lung adenocarcinoma cells.[4] Although caffeine has been reported to modulate cell cycle checkpoints and perturb molecular targets of the cell cycle, the exact mechanism of caffeine-induced apoptosis remains unclear.[1]

Autophagy is a key mechanism in various physiopathological processes, including tumorigenesis, development, cell death and survival.[5,6] It has also been shown to have a complex relationship with apoptosis, especially in tumor cell lines.[7] Several reports have shown that autophagy not only enhances caspase-dependent cell death, but is also required for it.[8] In contrast, it has also been shown that autophagy plays an important role in promoting cell survival against apoptosis.[7] Caffeine has been reported to inhibit some kinase activities, including various forms of phosphoinositol-3 kinase and mammalian target of rapamycin (mTOR).[9,10] Recently, in food spoilage studies involving yeast, caffeine has been shown to induce a starvation response,[11] which is a key regulator of autophagy causing its induction. However, the exact mechanism by which caffeine induces autophagy is still unknown.

Here we report that higher concentrations of caffeine enhance autophagic flux in a dose-dependent manner in various cell lines. Furthermore, we show that caffeine-induced autophagy is mainly dependent on PI3K/Akt/mTOR/p70S6 signaling and eventually results in apoptosis.

*Correspondence to: Nobutaka Hattori; Email: nhattori@juntendo.ac.jp
Submitted: 06/22/10; Revised: 10/27/10; Accepted: 11/02/10
Previously published online: www.landesbioscience.com/journals/autophagy/article/14074
DOI:

Results and Discussion

Caffeine (**Fig. 1A**) is a widely used psychoactive drug that has been used for centuries to increase alertness and energy. It has been reported that caffeine induces autophagy in *Zygosaccharomyces bailii* in association with a starvation response, caused by a unknown mechanism.[11] However, it remains unknown whether caffeine affects autophagy in mammalian cells. To determine if caffeine regulates autophagy at a steady state, we first examined levels of the microtubule-associated protein 1 light chain 3 (LC3)-II, which is an LC3-phosphatidyl-ethanolamine conjugate and a promising autophagosomal marker.[12] LC3-II levels (compared to actin loading controls) increased with 5–25 mM caffeine treatment over 48 hours in SH-SY5Y (**Fig. 1B and C**), PC12D and HeLa cells (**Suppl. Fig. S1A and B**). The LC3-II/actin ratio also increased in a time-dependent manner in SH-SY5Y (**Fig. 1D and E**) and HeLa cells (data not shown). Using an electron microscopy technique, the numbers of autophagic vacuoles (AVs) were markedly increased in SH-SY5Y cells treated with 10 or 25 mM caffeine, but not in the control (**Fig. 1F and G**). Morphometric analysis revealed that the number of AVs per 100 μm^2 of SH-SY5Y cytoplasm in control (Mean ± standard deviation: 1.3 ± 0.50), whereas that in caffeine-treated cells (10 mM: 8.0 ± 0.82; 25 mM: 15 ± 1.9) for 24 hours. Expression levels of p62, a well-known autophagic substrate, were also decreased by caffeine treatment in SH-SY5Y (**Fig. 1H and I**) and HeLa cells (**Suppl. Fig. S1C and D**). Furthermore, 10 mM caffeine treatment markedly increased the number of EGFP-LC3-positive vesicles in SH-SY5Y cells transiently transfected with EGFP-LC3 (data not shown) and HeLa cells stably expressing EGFP-LC3 (**Figs. 1J and K**).[12,13] This effect was confirmed by the observation that caffeine administration also increased the number of vesicles positive to endogenous LC3 (**Suppl. Fig. S1E**).

Endogenous LC3 is post-transcriptionally processed into LC3-I, which is found in the cytosol. LC3-I is in turn lipidated to LC3-II, which then associates with autophagosome membranes.[14] LC3-II can accumulate due to increased upstream autophagosome formation or impaired downstream autophagosome-lysosome fusion. To distinguish between these two possibilities, we assayed LC3-II in the presence of E64D plus pepstatin A or bafilomycin A1, which inhibits lysosomal proteases or blocks downstream autophagosome-lysosome fusion and lysosomal proteases, respectively.[15,16] Caffeine significantly increased LC3-II levels in the presence of E64d plus pepstatin A or bafilomycin compared to E64d plus pepstatin A or bafilomycin alone in (**Fig. 2A and B; Suppl. Fig. S1F and G**) and HeLa cells (**Fig. 2C and D; Suppl. Fig. S1H and I**). A saturating dosage of bafilomycin A1 was used in this assay and no further increases in LC3-II levels were observed when cells were treated with higher concentrations. Similar results were observed in PC12D cell lines (data not shown). To confirm the caffeine effect on autophagic flux, we assessed the numbers of autolysosomes and autophagosomes in HeLa cells. The ratio of the numbers of autolysosomes (positive to both LC3 and LAMP2) to autophagosomes (positive to LC3) was increased by 10 mM caffeine treatment for 48 hours (**Fig. 2E**). Quantification data using ImageJ also showed significant increase of the ratio (**Fig. 2F**). These results strongly indicate that high concentration of caffeine treatment enhances autophagic flux.

The class I phosphatidylinositol 3-phosphate kinase (PI3K)/Akt/mTOR/p70ribosomal protein S6 kinase (p70S6K) signaling pathway and the Ras/Raf-1/mitogen-activated protein kinase 1/2 (MEK1/2)/extracellular signal-regulated kinase 1/2 (ERK1/2) pathway are two well-known pathways involved in the regulation of autophagy. Both are associated with tumorigenesis and often activated in numerous types of tumors.[17] Therefore, we examined the effect of caffeine on both of these pathways, using western blotting, according to the protocol by Inoki and colleagues.[18] After a 24 hour treatment with caffeine, there was a significant decrease in the levels of phosphorylated p70 S6 kinase, S6 ribosomal protein and 4E-BP1, compared with total normal levels in SH-SY5Y (**Fig. 3A**), HeLa and PC12D cells (data not shown). Consistent with these results, nonphosphorylated 4E-BP1 proteins were increased by caffeine treatment (**Fig. 3A**). To further investigate the upstream inhibition of mTOR by caffeine, we examined Ser473 phosphorylation of Akt, which measures both Akt/mTOR and mTORC2 activity. As shown in **Figure 3B**, treatment with caffeine also decreased the level of phosphorylated Akt in SH-SY5Y cells, which was consistent with a previous report.[19] Similar findings were obtained in HeLa (**Suppl. Fig. S2A**) and PC12D cells (data not shown). Subsequently, we examined whether caffeine increases the phosphorylation of ERK1/2, a key regulator of autophagy downstream of Akt. As shown in **Figure 3C**, treatment with caffeine increased phosphorylated ERK1/2. The effects of caffeine on mTOR inhibition were initially detected 3 hours after the addition of caffeine and reached a maximal level after 6 hours in SH-SY5Y (**Fig. 3D**) and 9 hours in HeLa cells (**Suppl. Fig. S2B and C**).

Caffeine has been shown to inhibit PI3K and components of the PI3K/Akt pathway.[9,20] Next, we performed experiments to confirm whether caffeine-induced autophagy is activated through the PI3K/Akt pathway. Insulin or insulin-like growth factor upregulates PI3K and its downstream targets including Akt and mTOR, resulting in the inactivation of autophagy.[21-23] As shown in **Figure 4A and B**, insulin treatment for 30 minutes significantly phosphorylated Akt at Ser473, whereas the phosphorylation was completely abolished by additional treatment with caffeine. No significant differences of the LC3-II/

Figure 1A–G (See opposite page). Caffeine increases autophagic flux in various cell lines. (A) Structural formula of caffeine. (B and C) SH-SY5Y cells treated with various concentrations of caffeine for 24 or 48 hours were analyzed by immunoblotting (B) with antibodies against LC3 and actin. Densitometry analysis of LC3-II levels relative to actin (C) was performed using three independent experiments. (D and E) SH-SY5Y cells treated with 25 mM caffeine for 3–24 hours were analyzed by immunoblotting (D) with antibodies against LC3 and actin. Densitometry analysis of LC3-II levels relative to actin (E) was performed using three independent experiments. (F) Electron microscopic examination of SH-SY5Y cells treated with various concentrations of caffeine for 24 or 48 hours. Autophagic vacuoles accumulating in the cytoplasm are shown by arrows. (G) Morphometric analysis of autophagic vacuoles was performed with 30 different areas of the cytoplasm of control and caffeine-treated cells.

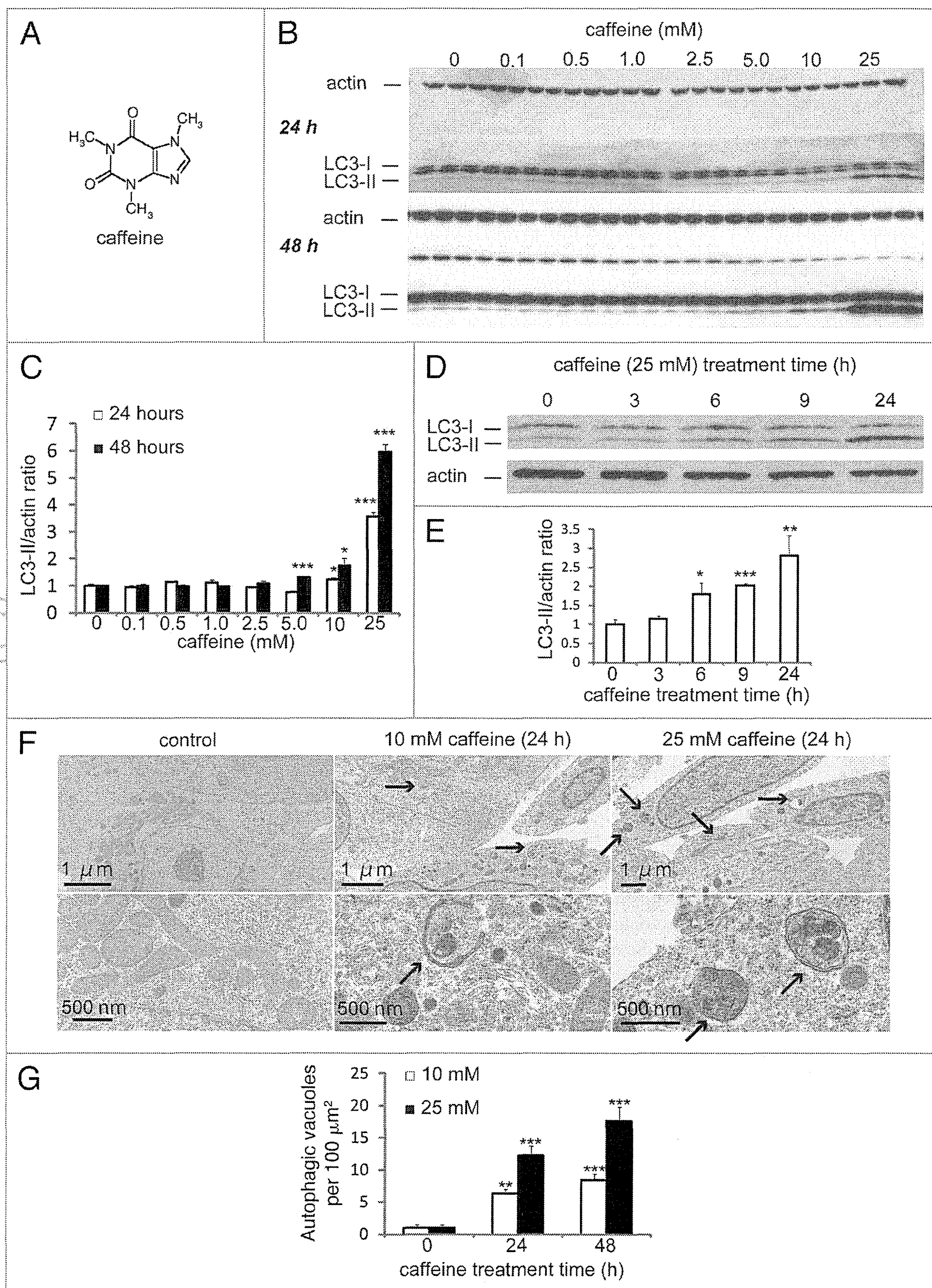

actin ratio between caffeine treatment and caffeine treatment with insulin were observed. Also, caffeine and Akt1/2 inhibitors did not have additive effects on the levels of LC3-II/actin ratio compared to the single treatment of caffeine or Akt inhibitors (**Fig. 4C and D**). To further confirm the caffeine effects on this pathway, cells were transiently transfected with myristoylated Akt (myr-Akt), a constitutively active form of Akt.[24] Caffeine treatment of both cells transfected with control vector and

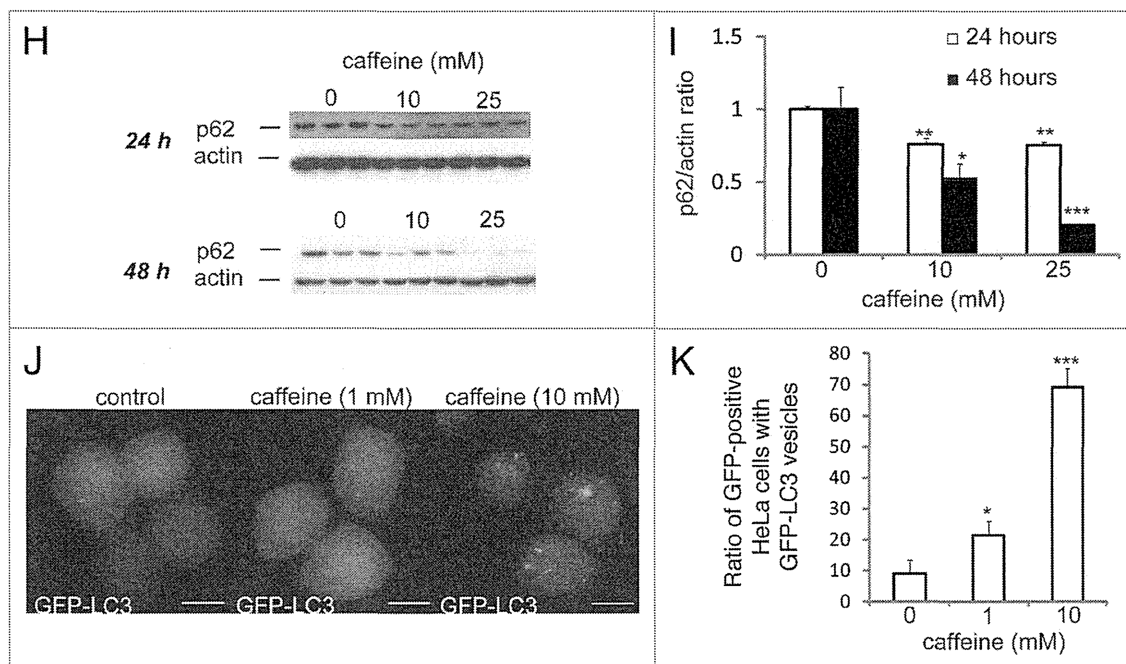

Figure 1H–K. Caffeine increases autophagic flux in various cell lines. (H and I) SH-SY5Y cells treated with various concentrations of caffeine for 24 or 48 hours were analyzed by immunoblotting with antibodies against p62 and actin. Densitometry analysis of p62 levels relative to actin (I) was performed using three independent experiments. (J and K) HeLa cells stably expressing EGFP-LC3 were treated with various concentrations of caffeine for 24 hours and analyzed using confocal microscopy. The percentage of EGFP-positive HeLa cells with >5 EGFP-LC3 vesicles was assessed (K) described previously in reference 43. Error bars, S.D.; $^{*}p < 0.05$; $^{**}p < 0.01$.

Do not distribute

myr-Akt markedly decreased the levels of the phosphorylated Akt (Fig. 3E), indicating that caffeine directly inhibits the Akt phosphorylation. If caffeine facilitates autophagy through PI3K/Akt and ERK1/2 signalings, the autophagy should be partially blocked by ERK1/2 inhibition using the mitogen-activated protein kinase kinase 1/2 (MEK1/2) inhibitor, U0126. U0126 significantly but mildly reversed the levels of LC3-II/actin ratio (**Fig. 4F and G**). The failure of U1026 to reverse completely the caffeine effect can be explained by the autophagy induction through Akt/mTOR signaling. In addition, only Akt knockdown with inducible short hairpin RNAs (shRNAs) to specifically and stably knock down all three Akt isoforms sufficiently increases autophagic flux.[25] Therefore, we concluded that the caffeine-induced autophagy is mainly dependent on the PI3K/Akt/mTOR pathway.

Because caffeine induces autophagy dependently of mTOR inhibition, we hypothesized that combination treatment of caffeine with rapamycin would not have additive effects on autophagy. However, caffeine and rapamycin showed an additive effect on the enhancement of LC3-II/actin ratio compared to the single treatment of caffeine or rapamycin (**Fig. 5A and B**). Several lines of evidences support the hypothesis that resistance to rapamycin results from a positive feedback loop from mTOR/S6K1 to Akt, resulting in enhancement of Akt phosphorylation at Ser 473.[26-28] Recently, mutual suppression of the PI3K/Akt/mTOR pathway by combination of rapamycin with perifosine, an Akt inhibitor, induces synergistic effects on autophagy-induced apoptosis as well as enhancement of autophagy, suggesting that dual inhibition of the PI3K/Akt/mTOR by rapamycin with caffeine would be also a rational treatment for cancer.[29]

Several anti-cancer agents are known to inhibit the PI3K/Akt/mTOR/p70S6K pathway and simultaneously activate ERK1/2, resulting in induction of autophagy in tumor cell lines.[30,31] The upregulation of this process has beneficial effects in neurodegenerative diseases, such as Parkinson and Huntington diseases, whereas an excess of autophagy can lead to cell death.[32,33] Therefore, we decided to investigate whether caffeine-induced autophagy rescues or induces cell death. Using PC12D cells treated with 1-methyl-4-phenylpyridinium (MPP^+), a well-established Parkinson disease model,[34] we determined that 1 mM caffeine treatment was not sufficient for the induction of autophagy (**Suppl. Fig. S4 and B**) and promoted increased cell viability, whereas >2.5 mM caffeine decreased cell viability (**Fig. 6A**). In addition, a significant decrease in cell viability was noted in cells treated with >2.5 mM caffeine without MPP^+. Also, mitochondrial membrane potentials assessed by JC-1 were significantly preserved by 1 mM caffeine treatment compared to the control with MPP^+, while those were lost by >5 mM caffeine treatment (**Fig. 6B and Suppl. Fig. S5A**). These data suggest that caffeine-induced autophagy is not protective in these cell lines and leads to cell death.

Autophagy and apoptosis may act independently in parallel pathways or may influence one another.[7] To confirm the relationship between these pathways in cells treated with caffeine, we examined caffeine effects on the cell cycle with a propidium iodide (PI) staining assay. Treatment with 2.5–10 mM caffeine

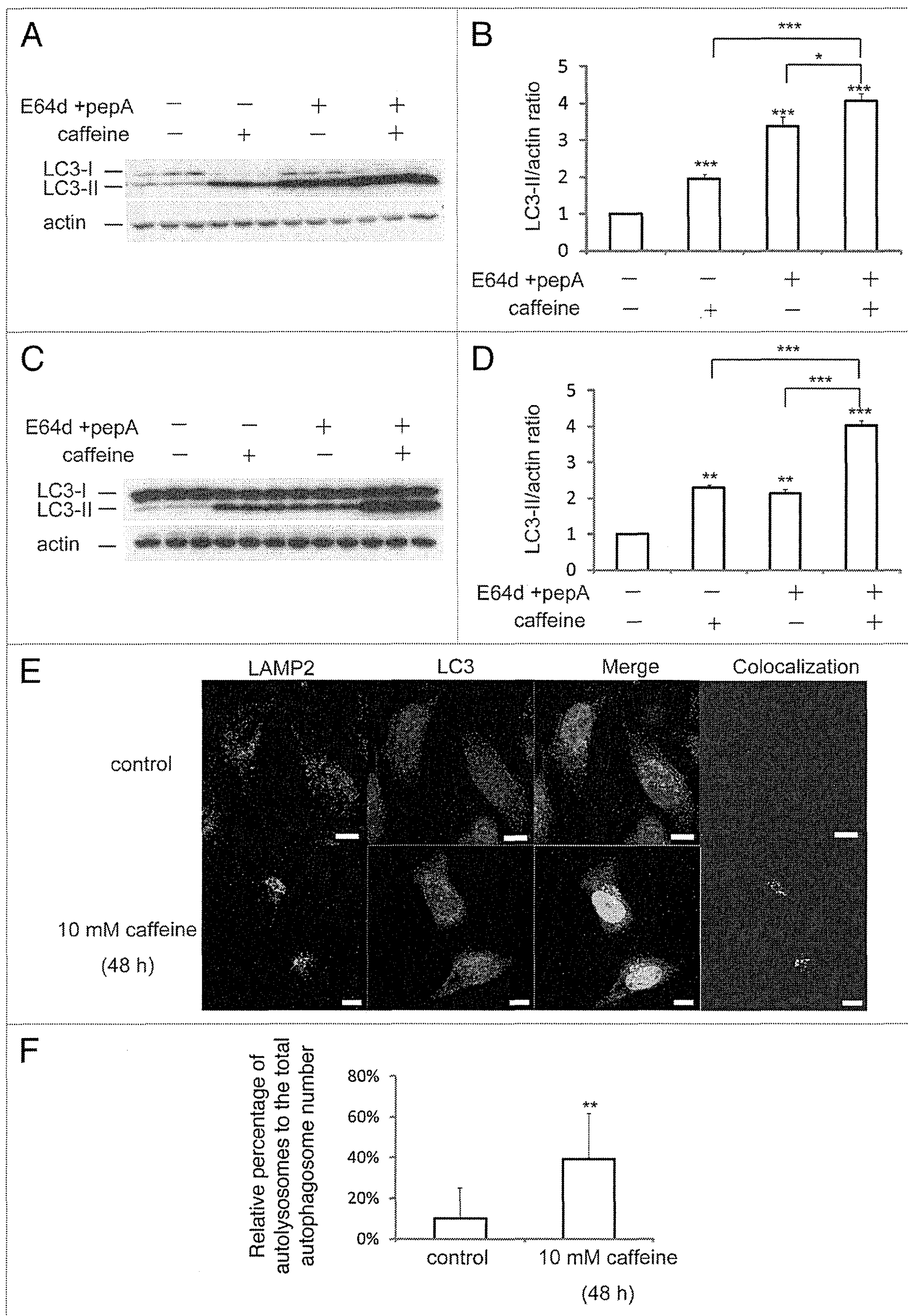

Figure 2. Caffeine does not block autophagosome-lysosome fusion. (A–D) SH-SY5Y (A) or HeLa (C) cells treated with 10 mM caffeine with or without E64d (10 μg/ml) and pepstatin A (10 μg/ml) were analyzed by immunoblotting with antibodies against LC3 and actin. Densitometry analysis of LC3 levels relative to actin in SH-SY5Y (B) and HeLa (D) cells was performed using three independent experiments. (E and F) HeLa cells treated with various concentrations of caffeine for 48 hours were analyzed using confocal microscopy (E). Number of the autolysosomes and autophagosomes were automatically counted using ImageJ "Colocalization" Plugin and the ratios were calculated (F).

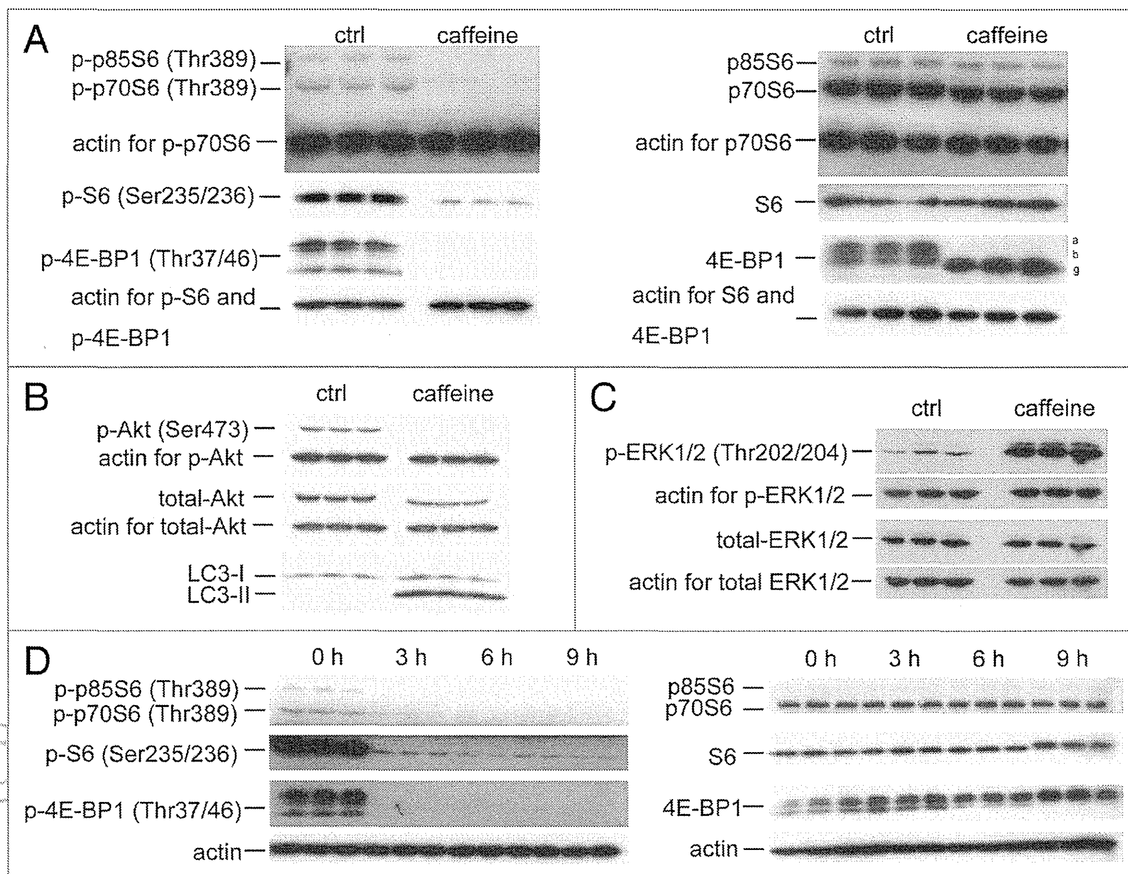

Figure 3. Caffeine inhibits the Akt/mTOR/p70S6 signaling pathway and activates ERK1/2 signaling. (A and B) SH-SY5Y cells treated with or without 10 mM caffeine for 24 hours were analyzed for mTOR activity by immunoblotting for levels of phosphor- and total p70 ribosomal S6 protein, S6, 4E-BP1 (A), Akt (B) and actin. (C) SH-SY5Y cells treated with or without 10 mM caffeine for 0, 3, 6 or 9 hours were analyzed by immunoblotting for levels of phosphor- and total ERK1/2 and actin. (D) SH-SY5Y cells treated with 10 mM caffeine for various time periods were analyzed by immunoblotting for levels of phosphor- and total p70 ribosomal S6 protein, S6, 4E-BP1 and actin.

increased the percentage of cells in the sub-G_1 peak, which is indicative of apoptosis (**Fig. 6C**). To confirm whether caffeine-induced cell death is apoptotic, we examined the activity of caspase-3, a well-known inducer of apoptosis. Treatment with 10 mM caffeine markedly increased levels of cleaved caspase-3 and decreased full-length caspase-3 in PC12D cells (**Fig. 6D**), consistent with previous reports on the induction of apoptosis by caffeine.[35-37]

To test whether caffeine-induced apoptosis is dependent on autophagy, we determined whether the inhibition of autophagy by 3-methyladenine (3-MA) or Atg7 siRNA knockdown affects caffeine-induced cytotoxicity in PC12D cells. Treatment with 1 or 5 mM 3MA or Atg7 knockdown significantly decreased the percentage of cell death or cells with reduced mitochondrial membrane potentials caused by caffeine treatment (5 or 10 mM) (**Fig. 6E and F and Suppl. Fig. S6B**). As can be seen from the increased caffeine-induced apoptosis shown in **Figure 6A and C**, our data suggests that caffeine-induced autophagy is necessary for apoptotic cell death. To further confirm this, we compared autophagy-deficient mouse embryonic fibroblasts (MEFs), lacking the Atg7 gene ($Atg7^{-/-}$), without LC3-II expression (**Suppl. Fig. S4E**), and matched wild-type ($Atg7^{+/+}$) MEFs, in which autophagy is induced by caffeine in a dose-dependent manner (**Suppl. Fig. S4C and D**). As expected, the level of caffeine-induced cell death (positive to trypan blue staining) in $Atg7^{-/-}$ MEFs was less than that in $Atg7^{+/+}$ MEFs (**Fig. 7A**). The numbers of early apoptotic cells (annexin V positive, PI negative) were significantly increased in both a time-dependent and dose-dependent manner by caffeine treatment of $Atg7^{+/+}$ MEFs compared to $Atg7^{-/-}$ MEFs (**Fig. 7B–D**). Also, apoptotic or necrotic cells (annexin V positive) were significantly increased by caffeine treatment of $Atg7^{+/+}$ MEFs compared to $Atg7^{-/-}$ MEFs (**Suppl. Fig. S6**). Together, these results indicate that caffeine-induced autophagy partly occurs upstream of apoptosis and is not a protective response to caffeine.

In various tumor cell lines, higher concentrations of caffeine alone induce p53-dependent G_1 phase arrest and under certain conditions apoptosis can also occur in a p53-independent manner.[1] Furthermore, disruption at the G_2/M checkpoint by caffeine allows cells time to repair DNA damage by driving them through mitosis, eventually resulting in apoptosis.[36,38,39] Consistent with these reports, the results of our study indicate that increased

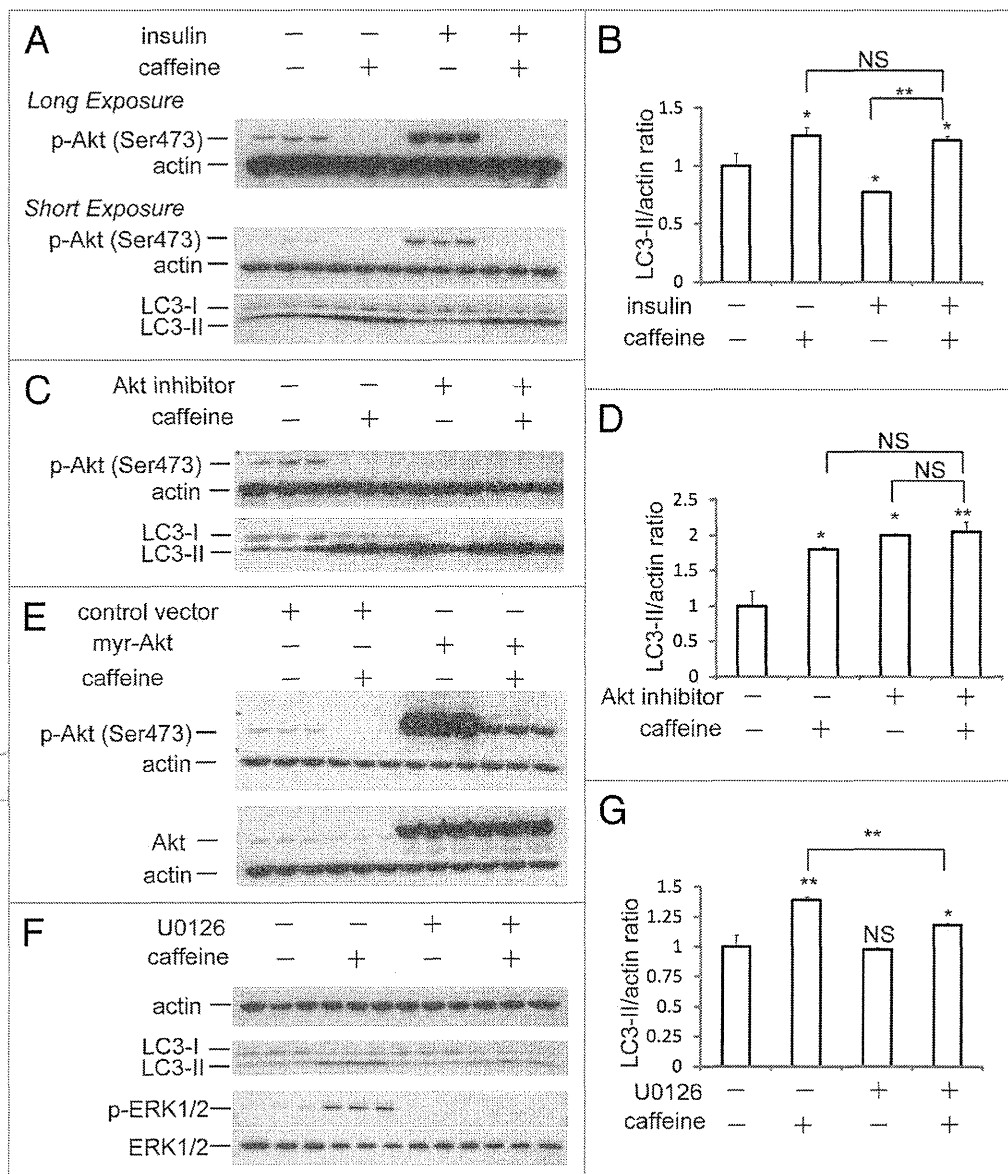

Figure 4. Caffeine-induced autophagy is dependent on PI3K/Akt/mTOR pathway. (A) SH-SY5Y cells treated with 25 mM caffeine for 3 hours followed by treatment with or without 200 nM insulin for 30 minutes were analyzed by immunoblotting. (B) Densitometry analysis of LC3-II levels relative to actin was performed using three independent experiments. (C) SH-SY5Y cells treated with 25 mM caffeine, 50 μM Akt1/2 inhibitors or 25 mM caffeine with 50 μM Akt1/2 inhibitors for 6 hours were analyzed by immunoblotting. (D) Densitometry analysis of LC3-II levels relative to actin was performed using three independent experiments. (E) SH-SY5Y cells were transfected for 24 hours with either a control plasmid DNA (pcDNA3.1) or a plasmid encoding constitutively active Akt (myr-Akt), and then treated with H_2O or 10 mM caffeine for 6 hours. Immunoblotting was performed using antibodies against Akt, p-Akt (Ser 473) and actin. (F) SH-SY5Y cells treated with 25 mM caffeine with or without 20 μM U0126 for 6 hours were analyzed by immunoblotting using antibodies against actin, LC3, p-ERK and ERK. (G) Densitometry analysis was performed using three independent experiments. Error bars, SD; $^*p < 0.05$; $^{**}p < 0.01$; N.S., not significant.

concentrations of caffeine treatment cause a dose-dependent increase in apoptosis. More recently, autophagy, a process long known to provide a survival advantage to cells undergoing nutrient deprivation and other stresses, has also been linked to the cell death process.[7] The cross-talk between apoptosis and autophagy is complex and sometimes contradictory; however, it is critical to the overall fate of the cell. In this study, we have shown that autophagy is induced by higher concentrations of caffeine without starvation, mainly via the inhibition of PI3K/Akt/mTOR/p70S6K signaling. Likewise, when caffeine-induced autophagy is blocked by 3-MA treatment or Atg7 knockout, apoptosis is partially attenuated, suggesting that caffeine-induced autophagy occurs upstream of caffeine-induced apoptosis. It also indicates the involvement of other pathways in caffeine-induced apoptosis. These results provide new insight into the effects of caffeine on cell death and survival and its use as a possible

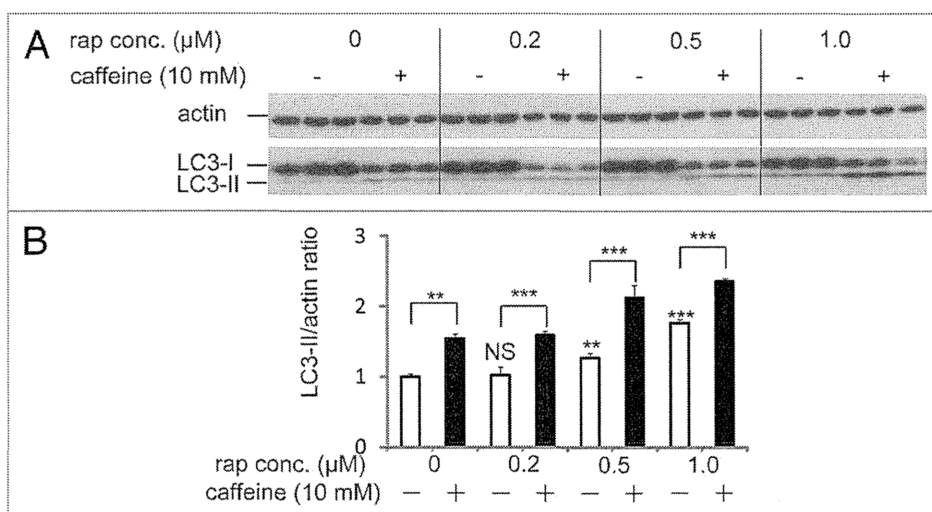

Figure 5. Rapamycin treatment with caffeine has an additive effect on enhancement of autophagy. (A) SH-SY5Y cells treated with various concentrations of rapamycin with or without 10 mM caffeine for 48 hours were analyzed by immunoblotting. (B) Densitometry analysis was performed using three independent experiments. Error bars, SD; *p < 0.05; **p < 0.01; N.S., not significant.

intervention strategy for the upregulation of apoptosis by a harnessing of its autophagic activity in tumor treatment.

Materials and Methods

Cell line. HeLa cells were maintained in DMEM (Sigma) supplemented with 10% fetal bovine serum (FBS) (Sigma) and 100 U/ml penicillin/streptomycin (Sigma) at 37°C and 5% CO_2. PC12D and SH-SY5Y cells were maintained in DMEM (Sigma) supplemented with 10% FBS (Sigma), 5% horse serum and 100 U/ml penicillin/streptomycin at 37°C and 5% CO_2. All experiments with PC12D were performed after differentiation with NGF treatment for 48 hours. Atg7$^{+/+}$ and $^{-/-}$ MEFs were maintained in DMEM (Sigma) supplemented with 10% FBS, 100 U/ml penicillin/streptomycin, 1% sodium pyruvate (Gibco, 11360), 1% non-essential amino acid (NEAA) and 4.2 μl 2% beta-mercaptoethanol at 37°C.

To establish a HeLa GFP-LC3 stable cell line, proliferating HeLa cells were transfected with a GFP-LC3 plasmid.[14] Forty-eight hours post-transfection with Lipofectamine 2000 (Invitrogen), positive stable clones were selected by growing cells with G418 (400 μg/ml) for 2 weeks and maintained in DMEM (Sigma) supplemented with 10% FBS (Sigma), 100 U/ml penicillin/streptomycin and 200 μg/ml G418 at 37°C and 5% CO_2. All cellular experiments were performed with cells cultured in complete medium with FBS as explained above.

Cell viability assays. A trypan blue dye (Invitrogen, 15250-061) exclusion assay was used to examine cell viability and performed according to previously reported protocols.[40,41] Changes of mitochondrial membrane potentials were assessed also with the lipophilic cationic membrane potential-sensitive dye JC-1 (5,5',6,6'-tetrachloro-1,1',3,3'-tetraehylbenzimidazolylcarbocyanineiodide) (Wako, 106-00131) according to the manufacturer's protocol. Detection of early apoptotic cells was determined using an annexin V/propidium iodide (PI) detection kit (Invitrogen), according to the manufacturer's protocol. Briefly, 0.5 x 10^6 Atg7$^{+/+}$ or $^{-/-}$ MEFs were exposed to caffeine (0–25 mM) for 24 hours and washed twice. Then, they were incubated at room temperature with annexin V/Alexa488 and PI for 15 minutes. Annexin V$^+$PI$^-$ cells, considered as early apoptotic cells, were enumerated using FACScan (BD Biosciences). Data were analyzed with CellQuest (BD Biosciences) and FlowJo softwares (Tree Star Inc.). Cells positive or negative for annexin V were regarded as apoptotic or non-apoptotic cells, respectively.

Cell cycle analysis. To examine apoptosis, 1.0 x 10^4 cells/well PC12D cells were seeded onto 96-well culture plate and incubated for 48 h in DMEM with NGF and treated with caffeine for 72 h. The cells were harvested and washed with PBS and

Figure 6 (See opposite page). Caffeine induces apoptosis by enhancement of autophagy. (A) After PC12D cells were treated with 0, 1, 2.5, 5 or 10 mM caffeine with DMSO or MPP$^+$ for 72 hours, cell viability was measured using trypan blue dye exclusion assay. Data are the means of triplicate experiments. (B) After cells were treated with 0, 1, 2.5, 5 or 10 mM caffeine with DMSO or MPP$^+$ for 48 hours, mitochondrial membrane potential was analyzed by JC-1 using a flow cytometry. Data are the means of triplicate experiments. (C) After PC12D cells were treated with 0, 1, 2.5, 5 or 10 mM caffeine with DMSO or MPP$^+$ for 72 hours, caffeine-induced sub G_1 area was analyzed by propidium iodide staining assay using a flow cytometry. Data are the means of triplicate experiments. (D) PC12D cells were treated with H_2O or caffeine for 24 hours or staurosporine (positive control) for 3 hours and analyzed with immunoblotting for levels of caspase-3 and cleaved caspase-3. (E) After PC12D cells were treated with 0, 1, 2.5, 5 or 10 mM caffeine with or without 1, 3 or 5 mM 3MA for 24 hours, cell viability was measured by trypan blue dye exclusion assay. (F) PC12D cells were transfected with control siRNA or siRNAs targeting Atg7. Forty eight hours later, they were treated with 0, 1, 2.5 or 10 mM caffeine for 24 hours and mitochondrial membrane potential was analyzed using JC-1. The knockdown effects on Atg7 were confirmed by immunoblotting using antibodies against Atg7 and actin. Data are the means of triplicate experiments. Error bars, S.D. NS, not significant; *p < 0.05; **p < 0.01; ***p < 0.001.

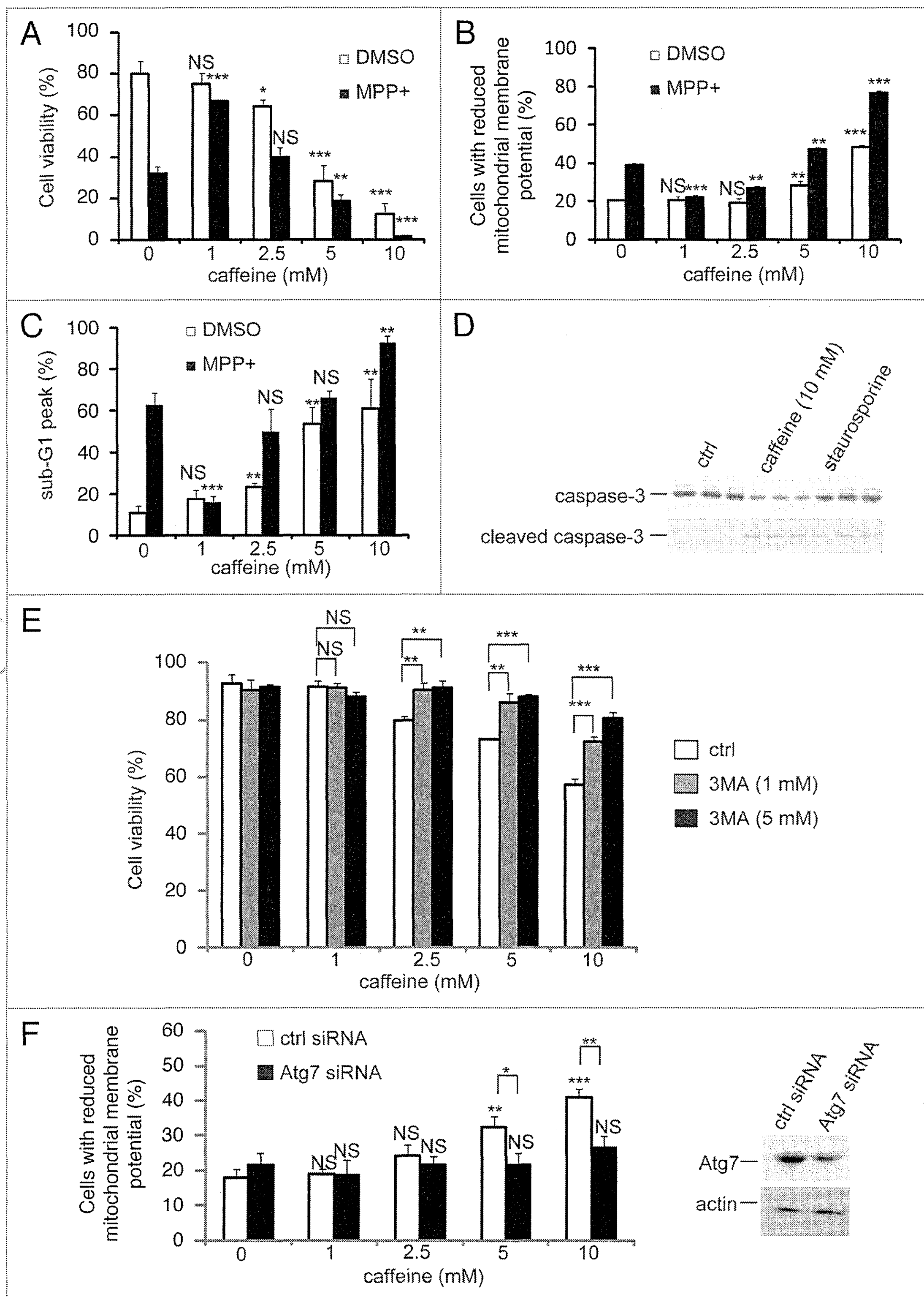

fixed with ice-cold 70% ethanol at 4°C for 2 h. The cells were then stained with PI solution according to previously reported protocol.[41] DNA content was analyzed by flow cytometry using FACScan and CellQuest software (BD Biosciences).

Compounds. Compounds used included caffeine (Wako, 031-06792), E64d (Sigma, E8640), pepstatin A (Sigma, P5318), rapamycin (LC Laboratories, R5000), CCI-779 (Selleck Chemicals, S1044), MPP+ (Sigma, M0896), bafilomycin A1 (Sigma, B1793), 3-methyladenine (Sigma, M9281), insulin (Sigma, I0516), U0126 (Sigma, U120), Akt1/2 inhibitors (Sigma, A6730), staurosporine (Cell Signaling Technology, 9953) and DMSO (Sigma, D2650).

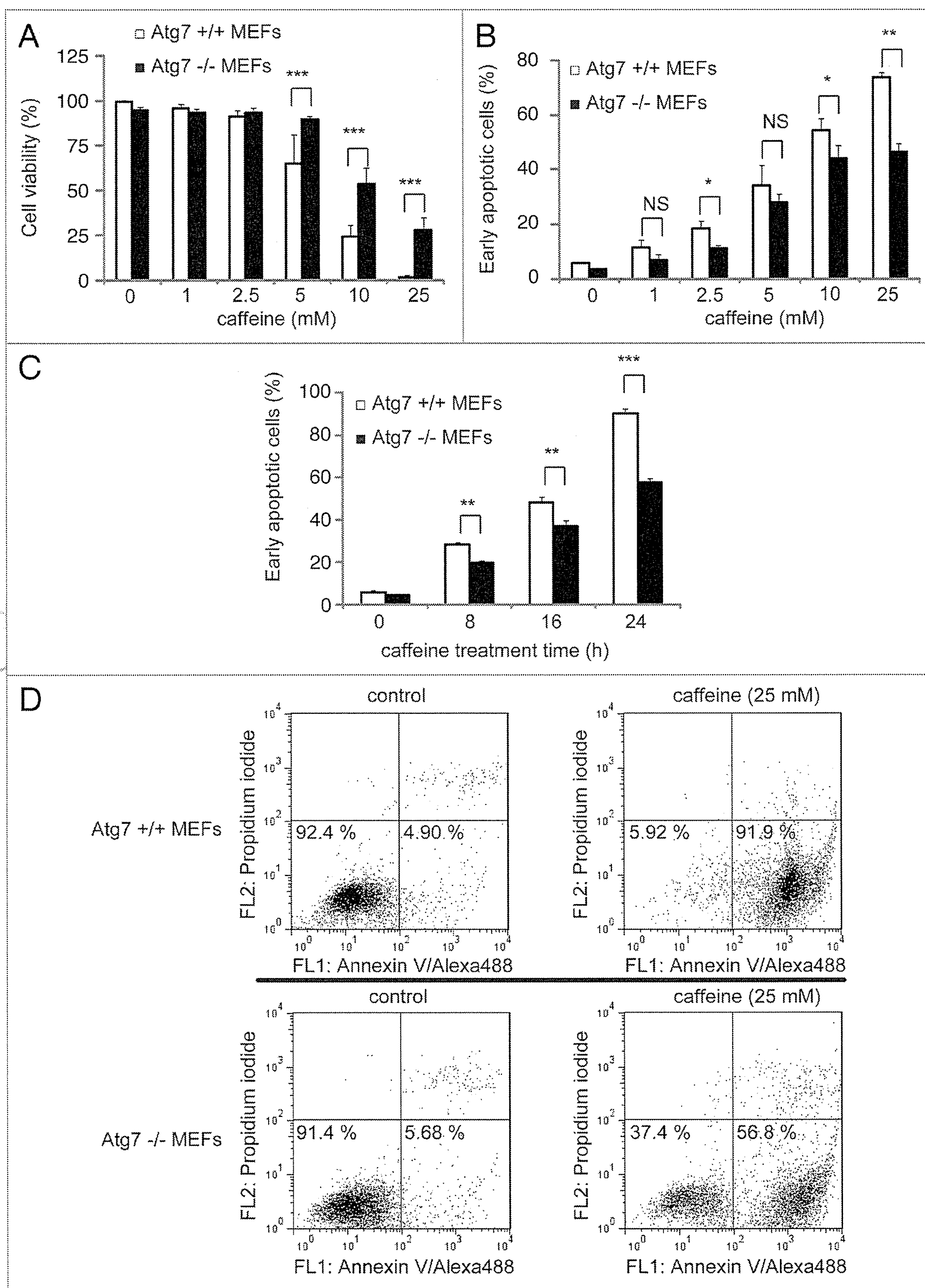

Figure 7. Cells without Atg7 expression are more resistant to caffeine-induced apoptosis. (A) After Atg7$^{+/+}$ or $^{-/-}$ mouse embryonic fibroblasts (MEFs) were treated with 0, 1, 2.5, 5, 10, 25 mM caffeine for 24 hours, the cell viability was measured by trypan blue dye exclusion assay. Data are the means of triplicate experiments. (B–D) Fluorescence-activated cell-sorting analysis for annexin V/propidium iodide (PI). Atg7$^{+/+}$ or $^{-/-}$ MEFs were cultured with various concentrations of caffeine for 24 hours (B) or with 25 mM caffeine for various times (0, 8, 16 or 24 hours) (C and D). Annexin V/PI staining was subsequently performed to assess early or late apoptosis and necrosis. 5 x 10^3 cells were analyzed by flow cytometry and the percentage of early apoptotic cells (annexin V-positive and PI-negative cells, the lower right region in (D) was determined). Data are the means of triplicate experiments. Error bars, SD. NS, not significant; *$p < 0.05$; **$p < 0.01$; ***$p < 0.001$.

Plasmid DNAs. Myrystoylated Akt (21–151), a constitutively active form of Akt, was purchased from Millipore.

siRNA knockdown experiments. PC12D cells were transfected with rat Atg7 siRNAs (Invitrogen, 10620318-9) using Lipofectamine RNAiMAX (Invitrogen, 13778-075) according to the manufacturer's protocol.

Western blotting. Cell pellets were lysed on ice in RIPA buffer for 20 minutes in the presence of protease inhibitor (Roche). Western blotting was performed according to a previously published report.[42] The antibodies used were as follows: anti-p70 ribosomal protein (Cell Signaling Technology, 2708), anti-ribosomal protein (Cell Signaling Technology, 2217), anti-4E-BP1 (Cell Signaling Technology, 9452), anti-Akt (Cell Signaling Technology, 9272), anti-p44/42 MAP kinase (Cell Signaling Technology, 9102), anti-phospho-p70 ribosomal protein (Thr389) (Cell Signaling Technology, 9205), anti-phospho-S6 ribosomal protein (Ser235/236) (Cell Signaling Technology, 2211), anti-phospho-4E-BP1 (Thr37/46) (Cell Signaling Technology, 9459), anti-phospho-p44/p42 MAPK (Thy202/Tyr204) (Cell Signaling Technology, 9101), anti-Atg7 (Cell Signaling Technology, 2631), anti-phospho-Akt (Cell Signaling Technology, 4060), anti-actin (Millipore, clone C4), anti-LC3 (MBL, clone 4E12), anti-p62 (Progen Biotechnik, GP62-C) antibodies. Antibody signals were enhanced with chemifluorescent methods from GE HealthCare.

Immunofluorescent microscopy. Cells were embedded with 4% paraformaldehyde for 20 minutes. Following this, they were permeabilized with 0.1% Triton-X in 1x PBS. After incubation with 10% FBS and 1% bovine serum albumin in 1x PBS for 30 minutes, cells were immunostained with anti-LC3B (x500) (Sigma, L7543), anti-LAMP2 (x50) (Development Studies Hybridoma Bank, clone H4B4) overnight and incubated with anti-rabbit IgG tagged with AlexaFluor 488 or anti-mouse IgG tagged with AlexaFluor 546 for 1 hour. The cover slips were embedded with VectaShield, stained with DAPI and images were acquired on a Zeiss LSM510 META confocal microscope (63 x 1.4 NA) or a Leica TCS SP5 confocal microscope at room temperature using Zeiss LSM510 v.3.2 software or Leica LAS AF software. Adobe Photoshop 7.0 (Adobe Systems Inc.) was used for subsequent image processing. For colocalization assay in HeLa cells, an appropriate confocal image was taken with Leica LAS AF software. Then, these images were analyzed automatically with the ImageJ "Colocalization" Plugin (Settings: Each threshold: 25, Ratio: 75%) followed by "Analyze particles" (Settings: threshold 25; Pixel: 1) between endogenous LC3 positive and LAMP2 vesicles. Experiments were done in triplicate at least twice.

Quantification of cells with GFP-LC3 vesicles. HeLa cells stable expressing GFP-LC3 were treated with various concentrations of caffeine for 24 or 48 hours and then fixed as described above. Analyses in triplicate were done for counting the proportion of GFP-positive cells with GFP-LC3 vesicles as previously described in reference 43.

Electron microscopy. SH-SY5Y cells treated with various concentrations of caffeine were prefixed in 2% glutaraldehyde in PBS at 4°C, treated with 1% OsO_4 for 3 hours at 4°C, dehydrated in a graded series of ethanol and flat embedded in epon. Ultra-thin sections were doubly stained with uranyl acetate and observed using a JEOL JEM-2000EX electron microscopy at 80 kV.

Statistical analysis. Densitometry analysis was performed using ImageJ 1.43 on immunoblots from three independent experiments. A t-test was performed with SYSTAT software (Hulinks).

Acknowledgements

We thank Dr. Takashi Ueno (Department of Biochemistry, Juntendo University) for critical comments and Drs. Masaaki Komatsu and Yu-Shin Sou for providing Atg7$^{+/+}$ and $^{-/-}$ MEFs. We are very grateful for a grant from Hayashi Memorial Foundation for Female Natural Scientists (Y.S.), the Grant-in-Aid for Young Scientists (B) (S. Saiki and F. Sato), grants from the All Japan Coffee Association (S. Saiki), the Takeda Scientific Foundation (S. Saiki) and the Nagao Memorial Fund (S. Saiki).

Note

Supplementary materials can be found at:
www.landesbioscience.com/supplement/SaikiAUTO7-2-Sup.pdf

References

1. Bode AM, Dong Z. The enigmatic effects of caffeine in cell cycle and cancer. Cancer Lett 2007; 247:26-39.
2. Jang MH, Shin MC, Kang IS, Baik HH, Cho YH, Chu JP, et al. Caffeine induces apoptosis in human neuroblastoma cell line SK-N-MC. J Korean Med Sci 2002; 17:674-8.
3. Gururajanna B, Al-Katib AA, Li YW, Aranha O, Vaitkevicius VK, Sarkar FH. Molecular effects of taxol and caffeine on pancreatic cancer cells. Int J Mol Med 1999; 4:501-7.
4. Qi W, Qiao D, Martinez JD. Caffeine induces TP53-independent G(1)-phase arrest and apoptosis in human lung tumor cells in a dose-dependent manner. Radiat Res 2002; 157:166-74.
5. Mizushima N, Levine B, Cuervo AM, Klionsky DJ. Autophagy fights disease through cellular self-digestion. Nature 2008; 451:1069-75.
6. Rubinsztein DC. The roles of intracellular protein-degradation pathways in neurodegeneration. Nature 2006; 443:780-6.
7. Eisenberg-Lerner A, Bialik S, Simon HU, Kimchi A. Life and death partners: apoptosis, autophagy and the cross-talk between them. Cell Death Differ 2009; 16:966-75.
8. Espert L, Denizot M, Grimaldi M, Robert-Hebmann V, Gay B, Varbanov M, et al. Autophagy is involved in T cell death after binding of HIV-1 envelope proteins to CXCR4. J Clin Invest 2006; 116:2161-72.
9. Foukas LC, Daniele N, Ktori C, Anderson KE, Jensen J, Shepherd PR. Direct effects of caffeine and theophylline on p110delta and other phosphoinositide 3-kinases. Differential effects on lipid kinase and protein kinase activities. J Biol Chem 2002; 277:37124-30.
10. Kudchodkar SB, Yu Y, Maguire TG, Alwine JC. Human cytomegalovirus infection alters the substrate specificities and rapamycin sensitivities of raptor- and rictor-containing complexes. Proc Natl Acad Sci USA 2006; 103:14182-7.
11. Winter G, Hazan R, Bakalinsky AT, Abeliovich H. Caffeine induces macroautophagy and confers a cytocidal effect on food spoilage yeast in combination with benzoic acid. Autophagy 2008; 4:28-36.
12. Rubinsztein DC, Cuervo AM, Ravikumar B, Sarkar S, Korolchuk V, Kaushik S, Klionsky DJ. In search of an "autophagomometer". Autophagy 2009; 5:585-9.
13. Tanida I, Ueno T, Kominami E. LC3 and Autophagy. Methods Mol Biol 2008; 445:77-88.
14. Kabeya Y, Mizushima N, Ueno T, Yamamoto A, Kirisako T, Noda T, et al. LC3, a mammalian homologue of yeast Apg8p, is localized in autophagosome membranes after processing. EMBO J 2000; 19:5720-8.
15. Yamamoto A, Tagawa Y, Yoshimori T, Moriyama Y, Masaki R, Tashiro Y. Bafilomycin A1 prevents maturation of autophagic vacuoles by inhibiting fusion between autophagosomes and lysosomes in rat hepatoma cell line, H-4-II-E cells. Cell Struct Funct 1998; 23:33-42.
16. Mizushima N, Yoshimori T, Levine B. Methods in mammalian autophagy research. Cell 140:313-26.
17. Hanahan D, Weinberg RA. The hallmarks of cancer. Cell 2000; 100:57-70.
18. Ikenoue T, Hong S, Inoki K. Monitoring mammalian target of rapamycin (mTOR) activity. Methods Enzymol 2009; 452:165-80.

19. Sinn B, Tallen G, Schroeder G, Grassl B, Schulze J, Budach V, Tinhofer I. Caffeine confers radiosensitization of PTEN-deficient malignant glioma cells by enhancing ionizing radiation-induced G_1 arrest and negatively regulating Akt phosphorylation. Mol Cancer Ther 9:480-8.
20. Sarkaria JN, Busby EC, Tibbetts RS, Roos P, Taya Y, Karnitz LM, Abraham RT. Inhibition of ATM and ATR kinase activities by the radiosensitizing agent, caffeine. Cancer Res 1999; 59:4375-82.
21. Inoki K, Li Y, Xu T, Guan KL. Rheb GTPase is a direct target of TSC2 GAP activity and regulates mTOR signaling. Genes Dev 2003; 17:1829-34.
22. Inoki K, Li Y, Zhu T, Wu J, Guan KL. TSC2 is phosphorylated and inhibited by Akt and suppresses mTOR signalling. Nat Cell Biol 2002; 4:648-57.
23. Garami A, Zwartkruis FJ, Nobukuni T, Joaquin M, Roccio M, Stocker H, et al. Insulin activation of Rheb, a mediator of mTOR/S6K/4E-BP signaling, is inhibited by TSC1 and 2. Mol Cell 2003; 11:1457-66.
24. Muise-Helmericks RC, Grimes HL, Bellacosa A, Malstrom SE, Tsichlis PN, Rosen N. Cyclin D expression is controlled post-transcriptionally via a phosphatidylinositol-3-kinase/Akt-dependent pathway. J Biol Chem 1998; 273:29864-72.
25. Degtyarev M, De Maziere A, Orr C, Lin J, Lee BB, Tien JY, et al. Akt inhibition promotes autophagy and sensitizes PTEN-null tumors to lysosomotropic agents. J Cell Biol 2008; 183:101-16.
26. Wan X, Harkavy B, Shen N, Grohar P, Helman LJ. Rapamycin induces feedback activation of Akt signaling through an IGF-1R-dependent mechanism. Oncogene 2007; 26:1932-40.
27. Sun SY, Rosenberg LM, Wang X, Zhou Z, Yue P, Fu H, Khuri FR. Activation of Akt and eIF4E survival pathways by rapamycin-mediated mammalian target of rapamycin inhibition. Cancer Res 2005; 65:7052-8.
28. O'Reilly KE, Rojo F, She QB, Solit D, Mills GB, Smith D, et al. mTOR inhibition induces upstream receptor tyrosine kinase signaling and activates Akt. Cancer Res 2006; 66:1500-8.
29. Cirstea D, Hideshima T, Rodig S, Santo L, Pozzi S, Vallet S, et al. Dual inhibition of akt/mammalian target of rapamycin pathway by nanoparticle albumin-bound-rapamycin and perifosine induces antitumor activity in multiple myeloma. Mol Cancer Ther 2010; 9:963-75.
30. Aoki H, Takada Y, Kondo S, Sawaya R, Aggarwal BB, Kondo Y. Evidence that curcumin suppresses the growth of malignant gliomas in vitro and in vivo through induction of autophagy: role of Akt and extracellular signal-regulated kinase signaling pathways. Mol Pharmacol 2007; 72:29-39.
31. Ellington AA, Berhow MA, Singletary KW. Inhibition of Akt signaling and enhanced ERK1/2 activity are involved in induction of macroautophagy by triterpenoid B-group soyasaponins in colon cancer cells. Carcinogenesis 2006; 27:298-306.
32. Rubinsztein DC, Gestwicki JE, Murphy LO, Klionsky DJ. Potential therapeutic applications of autophagy. Nat Rev Drug Discov 2007; 6:304-12.
33. Ravikumar B, Vacher C, Berger Z, Davies JE, Luo S, Oroz LG, et al. Inhibition of mTOR induces autophagy and reduces toxicity of polyglutamine expansions in fly and mouse models of Huntington disease. Nat Genet 2004; 36:585-95.
34. Korake Y, Ohta S. MPP+ analogs acting on mitochondria and inducing neuro-degeneration. Curr Med Chem 2003; 10:2507-16.
35. Hagan MP, Hopcia KL, Sylvester FC, Held KD. Caffeine-induced apoptosis reveals a persistent lesion after treatment with bromodeoxyuridine and ultraviolet-B light. Radiat Res 1997; 147:674-9.
36. Efferth T, Fabry U, Glatte P, Osieka R. Expression of apoptosis-related oncoproteins and modulation of apoptosis by caffeine in human leukemic cells. J Cancer Res Clin Oncol 1995; 121:648-56.
37. Shinomiya N, Takemura T, Iwamoto K, Rokutanda M. Caffeine induces S-phase apoptosis in cis-diamminedichloroplatinum-treated cells, whereas cis-diamminedichloroplatinum induces a block in G_2/M. Cytometry 1997; 27:365-73.
38. Lau CC, Pardee AB. Mechanism by which caffeine potentiates lethality of nitrogen mustard. Proc Natl Acad Sci USA 1982; 79:2942-6.
39. Takagi M, Shigeta T, Asada M, Iwata S, Nakazawa S, Kanke Y, et al. DNA damage-associated cell cycle and cell death control is differentially modulated by caffeine in clones with p53 mutations. Leukemia 1999; 13:70-7.
40. Ormerod MG, Collins MK, Rodriguez-Tarduchy G, Robertson D. Apoptosis in interleukin-3-dependent haemopoietic cells. Quantification by two flow cytometric methods. J Immunol Methods 1992; 153:57-65.
41. Kawatani M, Uchi M, Simizu S, Osada H, Imoto M. Transmembrane domain of Bcl-2 is required for inhibition of ceramide synthesis, but not cytochrome *c* release in the pathway of inostamycin-induced apoptosis. Exp Cell Res 2003; 286:57-66.
42. Kawajiri S, Saiki S, Sato S, Sato F, Hatano T, Eguchi H, Hattori N. PINK1 is recruited to mitochondria with parkin and associates with LC3 in mitophagy. FEBS Lett 2010; 584:1073-9.
43. Sarkar S, Davies JE, Huang Z, Tunnacliffe A, Rubinsztein DC. Trehalose, a novel mTOR-independent autophagy enhancer, accelerates the clearance of mutant huntingtin and alpha-synuclein. J Biol Chem 2007; 282:5641-52.

©2011 Landes Bioscience.
Do not distribute.

Neurobiology of Disease 41 (2011) 111–118

Contents lists available at ScienceDirect

Neurobiology of Disease

journal homepage: www.elsevier.com/locate/ynbdi

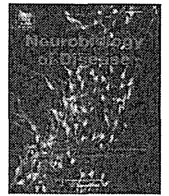

Mitochondrial membrane potential decrease caused by loss of PINK1 is not due to proton leak, but to respiratory chain defects

Taku Amo [a,1], Shigeto Sato [b], Shinji Saiki [b], Alexander M. Wolf [a], Masaaki Toyomizu [c], Clement A. Gautier [d], Jie Shen [d], Shigeo Ohta [a], Nobutaka Hattori [b,*]

[a] Department of Biochemistry and Cell Biology, Institute of Development and Aging Sciences, Graduate School of Medicine, Nippon Medical School, 1-396 Kosugi-cho, Nakahara-ku, Kawasaki 211-8533, Japan
[b] Department of Neurology, Juntendo University School of Medicine, 2-1-1 Hongo, Bunkyo-ku, Tokyo 113-8421, Japan
[c] Animal Nutrition, Life Sciences, Graduate School of Agricultural Science, Tohoku University, 1-1 Tsutsumidori-Amamiyamachi, Aoba-ku, Sendai 981-8555, Japan
[d] Center for Neurologic Diseases, Brigham and Women's Hospital, Program in Neuroscience, Harvard Medical School, Boston, MA 02115, USA

ARTICLE INFO

Article history:
Received 29 June 2010
Revised 17 August 2010
Accepted 25 August 2010
Available online 15 September 2010

Keywords:
Parkinson's disease
Mitochondria
PINK1
Parkin
Membrane potential
Oxidative phosphorylation
Modular kinetic analysis
Proton leak
Reactive oxygen species

ABSTRACT

Mutations in *PTEN-induced putative kinase 1* (*PINK1*) cause a recessive form of Parkinson's disease (PD). PINK1 is associated with mitochondrial quality control and its partial knock-down induces mitochondrial dysfunction including decreased membrane potential and increased vulnerability against mitochondrial toxins, but the exact function of PINK1 in mitochondria has not been investigated using cells with null expression of PINK1. Here, we show that loss of PINK1 caused mitochondrial dysfunction. In PINK1-deficient ($PINK1^{-/-}$) mouse embryonic fibroblasts (MEFs), mitochondrial membrane potential and cellular ATP levels were decreased compared with those in littermate wild-type MEFs. However, mitochondrial proton leak, which reduces membrane potential in the absence of ATP synthesis, was not altered by loss of PINK1. Instead, activity of the respiratory chain, which produces the membrane potential by oxidizing substrates using oxygen, declined. H_2O_2 production rate by $PINK1^{-/-}$ mitochondria was lower than $PINK1^{+/+}$ mitochondria as a consequence of decreased oxygen consumption rate, while the proportion (H_2O_2 production rate per oxygen consumption rate) was higher. These results suggest that mitochondrial dysfunctions in PD pathogenesis are caused not by proton leak, but by respiratory chain defects.

© 2010 Elsevier Inc. All rights reserved.

Introduction

Parkinson's disease (PD) is a neurodegenerative disease characterized by loss of dopaminergic neurons in the substantia nigra. Mitochondrial dysfunction has been proposed as a major factor in the pathogenesis of sporadic and familial PD (Abou-Sleiman et al., 2006). In particular, the identification of mutations in *PTEN-induced putative kinase 1* (*PINK1*) has strongly implicated mitochondrial dysfunction owing to its loss of function in the pathogenesis of PD (Valente et al., 2004). PINK1 contains an N-terminal mitochondrial targeting sequence (MTS) and a serine/threonine kinase domain (Valente et al., 2004). PINK1 kinase activity is crucial for mitochondrial maintenance via TRAP phosphorylation (Pridgeon et al., 2007). Loss of PINK1 function induces increased vulnerability to various stresses (Exner et al., 2007; Haque et al., 2008; Pridgeon et al., 2007; Wood-Kaczmar et al., 2008). However, silencing of PINK1 has only been partial and only one study has been performed to assess mitochondrial functions in steady and artificial states with complete ablation of PINK1 expression (Gautier et al., 2008).

Several studies have shown that PINK1 acts upstream of parkin in the same genetic pathway (Clark et al., 2006; Park et al., 2006) and co-overexpressed PINK1 and parkin both co-localized to mitochondria (Kim et al., 2008). Overexpression of PINK1 promotes mitochondrial fission (Yang et al., 2008). Fission followed by selective fusion segregates dysfunctional mitochondria and permits their removal by autophagy (Twig et al., 2008). PINK1 loss-of-function decreases mitochondrial membrane potential (Chu, 2010) and the PINK1–parkin pathway is associated with mitochondrial elimination in cultured cells treated with the mitochondrial uncoupler carbonyl cyanide *m*-chlorophenylhydrazone (CCCP), which causes mitochondrial depolarization (Geisler et al., 2010; Kawajiri et al., 2010; Matsuda et al., 2010; Narendra et al., 2008, 2010; Vives-Bauza et al., 2010). However, the exact mechanism underlying the mitochondrial depolarization induced by PINK1 defects leading to mitochondrial autophagy has not been examined in detail.

Abbreviations: $\Delta\psi$, mitochondrial membrane potential; FCCP, carbonyl cyanide *p*-trifluoromethoxyphenylhydrazone; MEFs, mouse embryonic fibroblasts; PD, Parkinson's disease; PINK1, PTEN-induced putative kinase 1; ROS, reactive oxygen species; TMRM, tetramethylrhodamine methyl ester; TPMP, triphenylmethylphosphonium.

* Corresponding author. Fax: +81 3 5800 0547.
E-mail address: nhattori@juntendo.ac.jp (N. Hattori).
[1] Present address: Department of Applied Chemistry, National Defense Academy, 1-10-20 Hashirimizu, Yokosuka 239-8686, Japan.

Available online on ScienceDirect (www.sciencedirect.com).

0969-9961/$ – see front matter © 2010 Elsevier Inc. All rights reserved.
doi:10.1016/j.nbd.2010.08.027

Here, we describe a detailed characterization of mitochondria in PINK1-deficient cells. We show that PINK1 deficiency causes a decrease in mitochondrial membrane potential, which is not due to proton leak, but to respiratory chain defects.

Materials and methods

PINK1 knock-out mouse embryonic fibroblasts (MEFs)

PINK1 knock-out MEFs were prepared and cultured as described previously (Matsuda et al., 2010). Mouse embryonic fibroblasts (MEFs) were derived from E12.5 embryos containing littermate 4 mice of each genotype. Embryos were mechanically dispersed by repeated passage through a P1000 pipette tip and plated with MEF media containing DME, 10% FCS, 1× nonessential amino acids, 1 mM L-glutamine, penicillin/streptomycin (invitrogen). The ψ2 cell line, an ecotropic retrovirus packaging cell line, was maintained in Dulbecco's modified Eagle medium (DMEM, Sigma) with 5% fetal bovine serum and 50 µg/ml kanamicin. Transfection of the ψ2 cells with pMESVTS plasmids containing an SV40 large T antigen was performed by lipofection method according to the manual provided by the manufacturer (GIBCO BRL). Five micrograms of the plasmids was used for each transfection. Transfectants were selected by G418 at the concentration of 0.5 mg/ml, and 10 clonal cell lines were established. The highest titer of 5×10^4 cfu/ml was obtained for the conditioned medium of a cell line designated ψ2SVTS1. 10^6 MEFs were plated onto a 10-cm culture dish and kept at 33 °C for 48 hours. Then medium was replaced with 2 ml supplemented with polybrene-supplemented medium conditioned by the ψ2SVTS1 cells at confluency for 3 days. Infection was continued for 3 hours, and the medium was replaced with a fresh one. The infected MEFs were cultured at 33 °C until immortalized cells were obtained.

We confirmed that the differences we detected in this study were due to the PINK1 deficiency, not to artificial effects by immortalization, by measuring cellular respiration rates of not immortalized MEFs from other littermates (Supplemental figure). The respiration rates of not immortalized MEFs were slightly slower than those of immortalized MEFs, but the differences between PINK1$^{+/+}$ and $^{-/-}$ MEFs were consistent (Fig. 2A).

Cell growth

Cells were seeded in 12-well plates at density of $3 \sim 6 \times 10^3$ cells/well and incubated in DMEM high glucose medium (4.5 g/l glucose and 1 mM sodium pyruvate) supplemented with 10% fetal bovine serum. After a day, the medium was replaced with DMEM glucose-free medium supplemented with 1 g/l galactose, 1 mM sodium pyruvate and 10% fetal bovine serum (DMEM galactose medium) at 37 °C in an incubator with a humidified atmosphere of 5% CO_2. Cells were trypsinized and live cells were assessed by trypan blue dye exclusion.

Mitochondrial morphological changes

Cells were seeded in 6-well plates at 2.0×10^5/well and incubated in DMEM high glucose medium (4.5 g/l glucose and 1 mM sodium pyruvate) supplemented with 10% fetal bovine serum and 1% penicillin/streptomycin. After a day, the medium was replaced with DMEM glucose-free medium supplemented with 1 g/l galactose, 1 mM sodium pyruvate and 10% fetal bovine serum (DMEM galactose medium) at 37 °C in an incubator with a humidified atmosphere of 5% CO_2. 24 hours later, cells were fixed and immunostained with anti-Tom20 antibody to visualize mitochondria according to a protocol as previously described (Kawajiri et al., 2010). All images were obtained using an Axioplan 2 imaging microscope (Carl Zeiss, Oberkochen, Germany).

Cellular ATP levels

Intracellular ATP levels were determined by a cellular ATP assay kit (TOYO B-Net, Tokyo, Japan) according to the manufacturer's instructions using a Lumat LB9507 luminometer (Berthold Technology, Bad Wildbad, Germany).

Membrane potential

Fluorescence images were recorded using a multi-dimensional imaging workstation (AS MDW, Leica Microsystems, Wetzlar, Germany) with a climate chamber maintained at 37 °C. Fluorescence was quantified with a CCD camera (CoolSnap HQ, Roper Scientific, Princeton, NJ) using a 20× objective. Cells were stained for 1 hour with a non-quenching concentration (20 nM) of tetramethylrhodamine methyl ester (TMRM) in a 96-well plate. The cell-permeable cationic dye TMRM accumulates in mitochondria according to the Nernst equation. Nuclei were stained with 250 nM Hoechst 34580. Mitochondrial TMRM fluorescence was integrated in a 40-µm diameter circular area around the nucleus, and the minimum fluorescence in this area was subtracted as background fluorescence.

Cell respiration

Cell respiration was measured at 37 °C using the Oxygen Meter Model 781 and the Mitocell MT200 closed respiratory chamber (Strathkelvin Instruments, North Lanarkshire, United Kingdom). Cells were cultured in DMEM with 4.5 g/l of glucose supplemented with 10% FBS. Cells were then trypsinized and resuspended in Leibovitz's L-15 medium (Invitrogen) at density of 8.0×10^6 cells/ml. The oxygen respiration rate was measured under each of the following three conditions: basal rate (no additions); State 4 (no ATP synthesis) [after addition of 1 µg/ml oligomycin (Sigma)], uncoupled [after addition of 3 µM FCCP (carbonyl cyanide *p*-trifluoromethoxyphenylhydrazone; Sigma)] using Strathkelvin 949 Oxygen System. After sequential measurements, the endogenous respiration rate was determined by adding 1 µM rotenone + 2 µM myxothiazol.

Mitochondrial respiration and membrane potential

Mitochondria were prepared from cultured MEFs as previously described (Amo and Brand, 2007). Mitochondrial oxygen consumption with 5 mM succinate as a respiratory substrate was measured at 37 °C using a Clark electrode (Rank Brothers, Cambridge, United Kingdom) calibrated with air-saturated respiration buffer comprising 0.115 M KCl, 10 mM KH_2PO_4, 3 mM HEPES (pH 7.2), 2 mM $MgCl_2$, 1 mM EGTA and 0.3% (w/v) defatted BSA, assumed to contain 406 nmol atomic oxygen/ml (Reynafarje et al., 1985). Mitochondrial membrane potential ($\Delta\psi$) was measured simultaneously with respiratory activity using an electrode sensitive to the lipophilic cation $TPMP^+$ (triphenylmethylphosphonium) (Brand, 1995). Mitochondria were incubated at 0.5 mg/ml in the presence of 80 ng/ml nigericin (to collapse the pH gradient so that the proton motive force was expressed exclusively as $\Delta\psi$) and 2 µM rotenone (to inhibit complex I). The $TPMP^+$-sensitive electrode was calibrated with sequential additions of $TPMP^+$ up to 2 µM, then 5 mM succinate was added to initiate respiration. Experiments were terminated with 2 µM FCCP, allowing correction for any small baseline drift. $\Delta\psi$ was calculated from the distribution of $TPMP^+$ across the mitochondrial inner membrane using a binding correction factor of 0.35 mg protein/µl. Respiratory rates with 4 mM pyruvate + 1 mM malate as a substrate in State 3 (with 0.25 mM ADP) and State 4 (with 1 µg/ml oligomycin) were determined using the Oxygen Meter Model 781 and the Mitocell MT200 closed respiratory chamber (Strathkelvin Instruments).

Modular kinetic analysis

To investigate differences in oxidative phosphorylation caused by PINK1 knock-out, we applied a systems approach, namely modular kinetic analysis (Amo and Brand, 2007; Brand, 1990). This analyzes the kinetics of the whole of oxidative phosphorylation divided into three modules connected by their common substrate or product, $\Delta\psi$. The modules are (i) the reactions that produce $\Delta\psi$, consisting of the substrate translocases, dehydrogenases and other enzymes and the components of the respiratory chain, called 'substrate oxidation'; (ii) the reactions that consume $\Delta\psi$ and synthesize, export and dephosphorylate ATP, consisting of ATP synthase, the phosphate and adenine nucleotide translocases and any ATPases that may be present, called the 'phosphorylating system'; and (iii) the reactions that consume $\Delta\psi$ without ATP synthesis, called the 'proton leak' (Brand, 1990). The analysis reports changes anywhere within oxidative phosphorylation that are functionally important but is unresponsive to changes that have no functional consequences. Comparison of the kinetic responses of each of the three modules to $\Delta\psi$ obtained using mitochondria isolated from PINK1$^{+/+}$ and PINK1$^{-/-}$ MEFs would reveal any effects of PINK1 on the kinetics of oxidative phosphorylation. Oxygen consumption and $\Delta\psi$ were measured simultaneously using mitochondria incubated with 80 ng/ml nigericin and 4 μM rotenone. Respiration was initiated by 5 mM succinate. The kinetic behavior of a '$\Delta\psi$-producer' can be established by specific modulation of a $\Delta\psi$-consumer and the kinetics of a consumer can be established by specific modulation of a $\Delta\psi$-producer (Brand, 1998). To measure the kinetic response of proton leak to $\Delta\psi$, the State 4 (non-phosphorylating) respiration of mitochondria in the presence of oligomycin (0.8 μg/ml; to prevent any residual ATP synthesis), which was used solely to drive the proton leak, was titrated with malonate (up to 8 mM). In a similar way, State 4 respiration was titrated by FCCP (up to 1 μM) for measurement of the kinetic response of substrate oxidation to $\Delta\psi$. State 3 (maximal rate of ATP synthesis) was obtained by addition of excess ADP (1 mM). Titration of State 3 respiration with malonate (up to 1.1 mM) allowed measurement of the kinetics of the $\Delta\psi$-consumers (the sum of the phosphorylating system and proton leak). The coupling efficiencies of oxidative phosphorylation were calculated from the kinetic curves as the percentage of mitochondrial respiration rate at a given $\Delta\psi$ that was used for ATP synthesis and was therefore inhibited by oligomycin. Note that any slip reactions will appear as proton leak in this analysis (Brand et al., 1994).

Mitochondrial ROS production

Mitochondrial ROS production rate was assessed by measurement of H_2O_2 generation rate, determined fluorometrically by measurement of oxidation of Amplex Red to fluorescent resorufin coupled to the enzymatic reduction of H_2O_2 by horseradish peroxidase using a spectrofluorometer RF-5300PC (Shimadzu, Kyoto, Japan). The H_2O_2 generation rate was measured in non-phosphorylating conditions (= State 4) using either pyruvate/malate or succinate as respiratory substrates. Mitochondria were incubated at 0.1 mg/ml in respiration buffer. All incubations also contained 5 μM Amplex Red, 2 U/ml horseradish peroxidase and 8 U/ml superoxide dismutase. The reaction was initiated by addition of 5 mM succinate or 4 mM pyruvate + 1 mM malonate and the increase in fluorescence was followed at excitation and emission wavelengths of 560 and 590 nm, respectively. Appropriate correction for background signals and standard curves generated using known amounts of H_2O_2 were used to calculate the rate of H_2O_2 production in nmol/min/mg mitochondrial protein. The percentage free radical leak, which is a measure of the number of electrons that produce superoxide (and subsequently H_2O_2) compared with the total number of electrons which pass thorough the respiratory chain, was calculated as the rate of H_2O_2 production divided by the rate of O_2 consumption (Barja et al., 1994).

Statistics

Values are presented as means ± SEM except Fig. 2D, in which error bars indicate SD. The significance of differences between means was assessed by the unpaired Student's *t*-test using Microsoft Excel; *P* values < 0.05 were taken to be significant.

Results

Cell growth and mitochondrial morphology

In general, cultured cells gain their energy mostly from glycolysis. Therefore, cells deficient in respiratory function can grow in normal medium, although possibly at a slower rate, relying predominantly on glycolysis (Hofhaus et al., 1996). Actually, ρ^0 cells, which lack mitochondrial DNA completely, can grow producing energy exclusively through glycolysis (King and Attardi, 1989). On the other hand, galactose metabolism via glycolysis is much slower than glucose metabolism (Reitzer et al., 1979). Therefore, cells in galactose medium are forced to oxidize pyruvate through the mitochondrial respiratory chain for energy required for growth. Consequently, cells with defects in their mitochondrial respiratory chains show growth impairments in galactose medium. To evaluate this phenomenon is also observed in our cells, we examined growth retardation by addition of mitochondrial complex I inhibitor, rotenone (Fig. 1A). In glucose medium, 10 nM rotenone had only a slight effect on the growth of PINK1$^{+/+}$ MEFs and slower growth was observed even in the presence of 100 nM rotenone. However, in the galactose medium, 10 nM rotenone significantly inhibited the growth of PINK1$^{+/+}$ MEFs and 100 nM roteone completely arrested the growth. Therefore, we could confirm that the growth impairment of our cells in the galactose medium was due to mitochondrial respiratory chain defects.

PINK1 acts upstream of parkin, regulating mitochondrial integrity and function; therefore, loss of PINK1 is considered to affect mitochondrial functions. To assess the mitochondrial functions of PINK1$^{-/-}$ MEFs, growth capability in a medium in which galactose replaced glucose was examined. As shown in Fig. 1B, PINK1$^{-/-}$ MEFs appeared to show clear growth impairments in the galactose medium, whereas PINK1$^{+/+}$ MEFs grew slightly slower than in the glucose medium.

No differences of mitochondrial morphology between PINK1$^{+/+}$ and $^{-/-}$ MEFs in the glucose medium were detected (Fig. 1C), consistent with the previous report (Matsuda et al., 2010). However, in the galactose medium, mitochondria of the PINK1$^{-/-}$ MEFs were more fragmented compared to the PINK$^{+/+}$ MEFs (Fig. 1C). This is consistent with previous reports, which found mitochondrial morphological changes were more pronounced when PINK1 knock-down HeLa cells were grown in low-glucose medium (Exner et al., 2007) and human PINK1 homozygous mutant fibroblast in galactose medium (Grünewald et al., 2009). In these cells, mitochondrial morphological changes were associated with the mitochondrial functional impairment.

Assessments of mitochondrial functions at the cellular level

Because PINK1$^{-/-}$ MEFs showed severe growth impairments in the galactose medium, the mitochondrial functions of these cells were assessed at the cellular level. First, cellular respiration rates were measured (Fig. 2A). The basal respiration rate was significantly reduced in PINK1$^{-/-}$ cells compared with that in PINK1$^{+/+}$ cells (11.13 ± 0.71 versus 14.36 ± 1.01 nmol O/min/10^6 cells; $p < 0.05$; $n = 5$ independent experiments), consistent with previous reports using partial knock-down of PINK1 expression (Gandhi et al., 2009; Liu et al., 2009). Oligomycin inhibits ATP synthase, resulting in non-phosphorylating respiration. FCCP uncouples oxidative phosphorylation, leading to maximum respiration rates. In both conditions, the

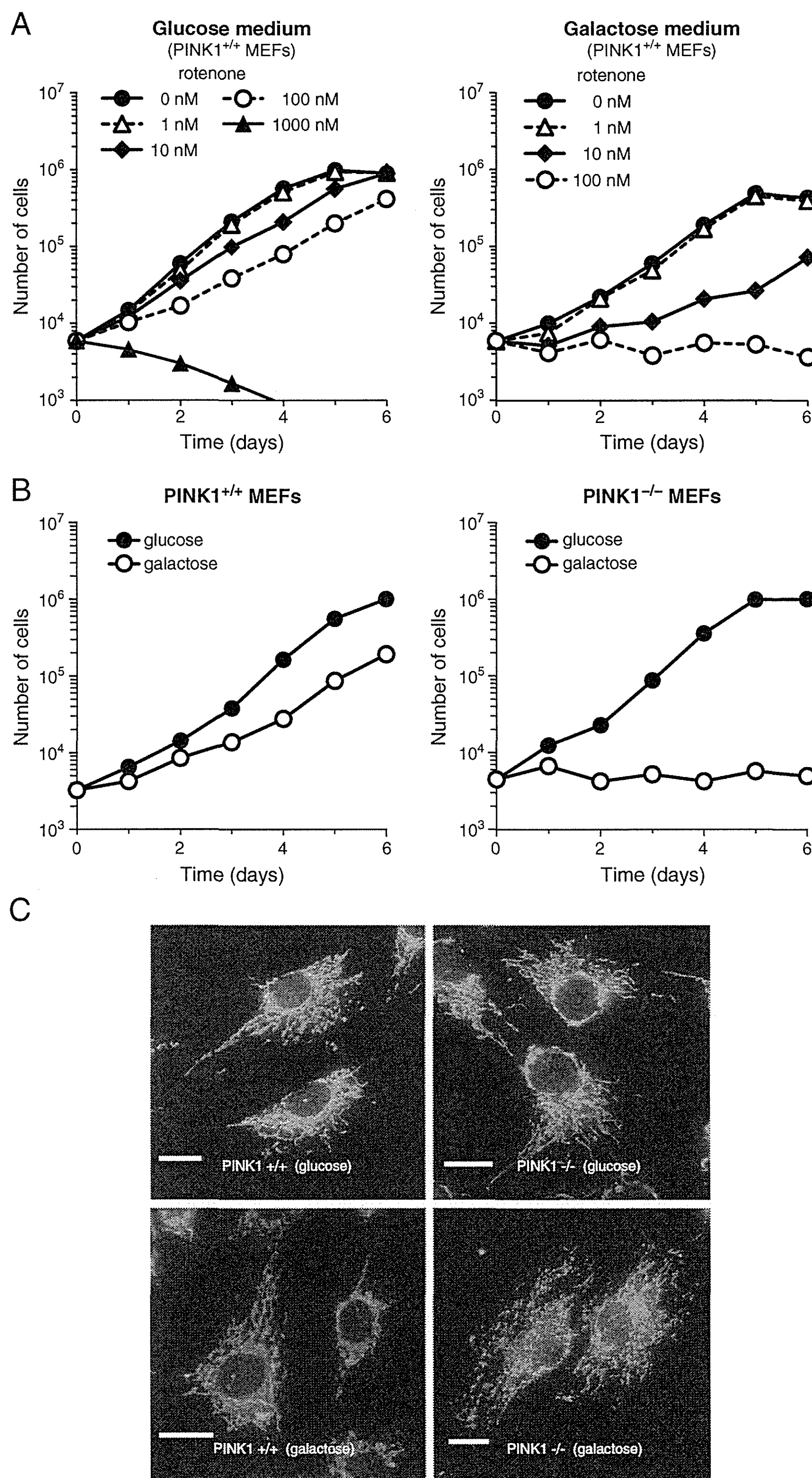

Fig. 1. (A) Growth retardation of PINK1$^{+/+}$ MEFs by mitochondrial complex I inhibitor, rotenone in glucose or galactose medium. Closed circles with solid line, 0 nM rotenone; open triangles with dashed line, 1 nM rotenone; closed diamonds with solid line, 10 nM rotenone; open circles with dashed line, 100 nM rotenone; closed triangles with solid line, 1000 nM rotenone. Cells grown in 12-well plates were trypsinized and live cells were assessed by trypan blue dye exclusion. (B) Growth curves of PINK1$^{+/+}$ and $^{-/-}$ MEFs. Closed symbols (*glucose*), growth curve for cells grown in DMEM containing 4.5 g/l glucose and 1 mM sodium pyruvate; open symbols (*galactose*), growth curve for cells grown in DMEM lacking glucose and containing instead 1.0 g/l galactose and 1 mM sodium pyruvate. Cells grown in 12-well plates were trypsinized and live cells were assessed by trypan blue dye exclusion. (C) Mitochondrial morphology of PINK1$^{+/+}$ and $^{-/-}$ MEFs. After incubating cells with the glucose or galactose medium for 24 hours, cells were fixed and immunostained with anti-Tom20 antibody to visualize mitochondria. Scale bar, 20 μm.

PINK1$^{-/-}$ cells respired significantly slower than the PINK1$^{+/+}$ cells (1.76 ± 0.13 versus 2.95 ± 0.27 ($p<0.01$; $n=5$ independent experiments) and 16.44 ± 1.80 versus 23.50 ± 1.18 nmol O/min/10^6 cells ($p<0.05$; $n=5$ independent experiments), respectively).

The main function of mitochondria is ATP synthesis via oxidative phosphorylation. ATP levels under basal conditions were significantly reduced in PINK1$^{-/-}$ MEFs (Fig. 2B), as reported previously for dissociated PINK1$^{-/-}$ mouse neurons (Gispert et al., 2009) and PINK1

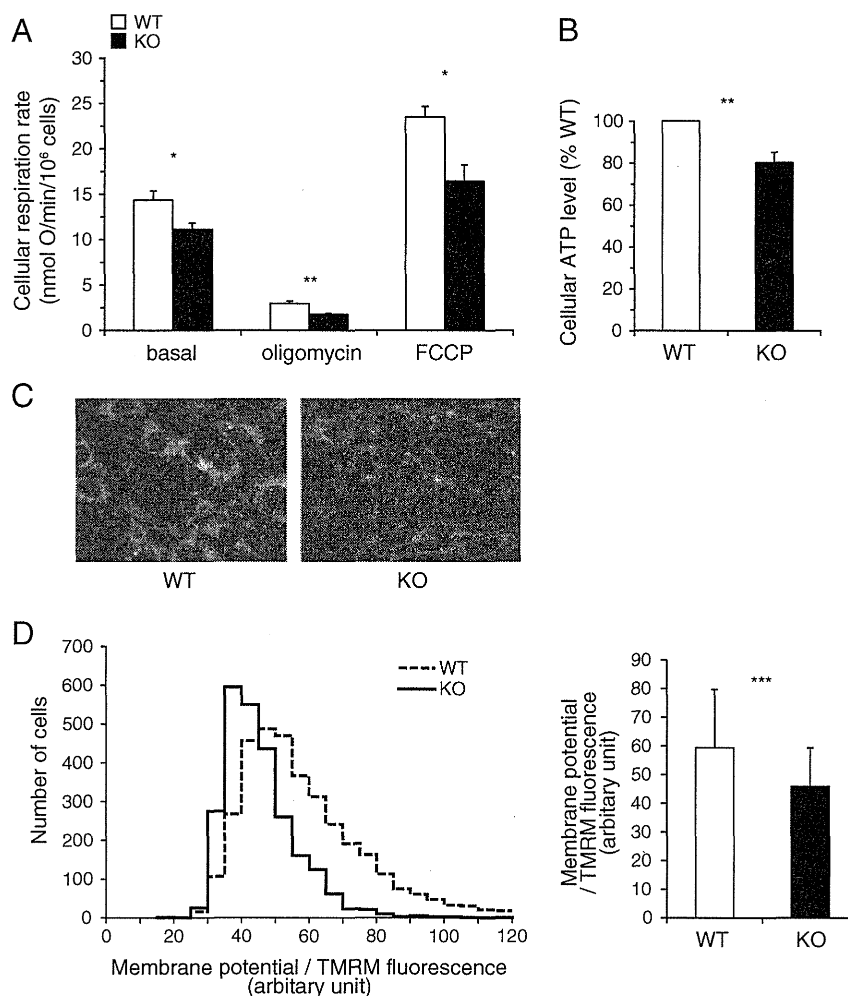

Fig. 2. Mitochondrial functions assessed at the cellular level. Open bars, PINK1$^{+/+}$ MEFs; closed bars, PINK1$^{-/-}$ MEFs. (A) Cell respiration rate of PINK1$^{+/+}$ and $^{-/-}$ MEFs. The oxygen respiration rate was measured at density of 8.0×10^6 cells/ml under each of the following three conditions: basal rate (no additions); State 4 (no ATP synthesis) [after addition of 1 μg/ml oligomycin], uncoupled [after addition of 3 μM FCCP]. After sequential measurements, the endogenous respiration rate was determined by adding 1 μM rotenone + 2 μM myxothiazol. Error bars indicate SEM ($n = 5$ independent experiments). (B) Cellular ATP levels. Data were normalized based on cell numbers and expressed as the percentage of the level in PINK1$^{+/+}$ cells. Error bars indicate SEM ($n = 4$ independent experiments). (C) Live cell images of PINK1$^{+/+}$ and $^{-/-}$ MEFs with TMRM fluorescence. (D) Mitochondrial membrane potential evaluated by live cell imaging of TMRM fluorescence. *Left panel*, the distribution of TMRM fluorescence from 3537 PIINK1$^{+/+}$ and 2566 PINK1$^{-/-}$ cells from 12 wells per cell type; *right panel*, the average value of TMRM fluorescence per cell. Error bars indicate SD. *$P<0.05$; **$P<0.01$; ***$P<0.001$.

siRNA knock-down PC12 cells (Liu et al., 2009). Mitochondrial membrane potential was also measured by live cell imaging of TMRM fluorescence. Typical images were shown in Fig. 2C. The histogram shows the distribution of TMRM fluorescence from 3537 PINK1$^{+/+}$ cells and 2566 PINK1$^{-/-}$ cells from 12 wells per cell type and the bar graph indicates the mean ± SD of TMRM fluorescence per cell (Fig. 2D). According to the Nernst equation, the ratio of TMRM fluorescence would translate into, on average, 6.88 mV lower mitochondrial membrane potential in the PINK1$^{-/-}$ cells if the plasma membrane potentials were not different between PINK1$^{+/+}$ and $^{-/-}$ cells. Mitochondrial membrane potential decrease was also showed previously in PINK1 knock-down HeLa cells (Exner et al., 2007) and in stable PINK1 knock-down neuroblastoma cell lines (Sandebring et al., 2009).

Assessments of mitochondrial functions using isolated mitochondria

To further analyze mitochondrial functions, we measured the kinetics of oxidative phosphorylation using isolated mitochondria from PINK1$^{+/+}$ and $^{-/-}$ MEFs. Fig. 3 shows the kinetics of the three modules of oxidative phosphorylation using succinate as a respiratory substrate (complex II-linked respiration). Fig. 3A shows the kinetic response of substrate oxidation to its product, $\Delta\psi$. The substrate oxidation kinetic curve for PINK1$^{-/-}$ cells was clearly shifted lower compared with that for PINK1$^{+/+}$ cells, indicating that the loss of PINK1 caused mitochondrial respiratory chain defects. Fig. 3B shows the kinetic response of proton leak to its driving force, $\Delta\psi$, and Fig. 3C shows the kinetic response of the ATP phosphorylating pathway to its driving force, $\Delta\psi$. Both kinetic curves for PINK1$^{+/+}$ and $^{-/-}$ MEFs (open and closed symbols, respectively) were overlapping, implying that there were no significant differences in those modules.

We also independently measured the mitochondrial oxygen consumption rate using pyruvate/malate as a respiratory substrate instead of succinate to check complex I. Modular kinetic analysis using pyruvate/malate is technically difficult for the following reasons: (1) the oxygen consumption rate with pyruvate/malate is much slower than succinate respiration; and (2) there are no competitive inhibitors of complex I-linked respiration, such as malonate for succinate respiration. As shown in Fig. 4A, the respiration rates in State 3 and 4 with pyruvate/malate of isolated mitochondria from PINK1$^{-/-}$ cells (closed symbols) were significantly slower than those of PINK1$^{+/+}$ cells (open symbols), as in the case of succinate respiration (Fig. 4B; data derived from the kinetic curves in Fig. 3).